Linköping University | Department of Electrical Engineerging
Master's thesis, 30 ECTS | Energy and Environmental Engineering
2023 | LIU-ISY/LITH-EX-A--2023/5584--SE

Techno-Economic Optimization and Control of Hybrid Energy Systems

An evaluation of control techniques in a large-scale system consisting of a battery energy storage system, photovoltaics, and an energy load including a fast charging station for electric vehicles

Louise Calmered
Tanja Nyberg

Supervisor : Robin Holmbom
Examiner : Christofer Sundström

LINKÖPING UNIVERSITY

Linköpings universitet
SE–581 83 Linköping
+46 13 28 10 00 , www.liu.se

Upphovsrätt

Copyright

Abstract

The increasing demand for renewable energy sources to meet climate targets and reduce carbon emissions poses challenges to the power grid due to their intermittent nature. One potential solution to maintain grid stability is by implementing Hybrid Energy Systems (HESs) that incorporate a Battery Energy Storage System (BESS). To achieve the most favorable outcome in terms of both technical feasibility and profitability of a BESS, it is essential to employ models for simulating and optimizing the control of system components.

This thesis focuses on the analysis of energy and revenue streams in a HES consisting of a BESS, photovoltaics (PVs), and an energy load including a fast charging station for electric vehicles (EVs). The objective is to optimize the system based on revenue generation by comparing the control techniques of peak shaving, energy arbitrage, and the integration of ancillary services within the Swedish energy market. The research questions explore the optimal utilization of the BESS and assess the impact of the different control techniques.

A model is created in Python with the package CasADi where data from an ongoing installation of a HES in southern Sweden is combined with data from literature research. The model includes an objective function that minimizes the total cost of power from the grid based on the day-ahead price, battery degradation, and monthly peak power.

To answer the research questions, four different scenarios are simulated. The first scenario is a base for comparison, the second one focuses on peak shaving and energy arbitrage, the third on participation in the ancillary service FCR-D upwards regulation, and the last one is a combination of peak shaving, energy arbitrage, and the ancillary service FCR-D. The results show that the remuneration from the ancillary service FCR-D is comparably much higher than the revenues generated from peak shaving and energy arbitrage, providing more than 500% of revenue compared to the same system but without a BESS. The scenario with peak shaving and energy arbitrage shows an increase in revenue of 29% but with more cycling of the battery which could cause losses in performance in the long term. To validate the results, sensitivity analyses are conducted by evaluating weighting in the objective function, implementing Model Predictive Control (MPC), and reviewing price variations.

In conclusion, efficient control techniques can enhance system performance, minimize losses, and ensure optimal utilization of different energy sources, leading to improved feasibility and profitability. The optimal usage of a BESS involves finding a balance between maximizing revenue generation and minimizing battery degradation. This can be achieved through control strategies that optimize the charging and discharging patterns of the BESS based on electricity price signals, demand patterns, and battery health considerations.

Acknowledgments

This master thesis marks the end of our studies at Linköping University and the Master of Science Programme in Energy - Environment and Management, with a specialization in Technology for Sustainable Development.

We have contributed equally to the production of this study, working together on the modeling as well as the report. However, Louise has had greater responsibility for the Background, and the Design of the optimization model, and Tanja for conducting the simulations. We thank each other for great teamwork and hope that our roads come to cross in the future.

We would like to express our gratitude to everyone that has been supporting us throughout the study, and the warmest thanks to the supervisor and colleagues at the collaborating energy company, who contributed to our work by sharing knowledge, and data, and providing feedback.

Our sincere appreciation goes to Robin Holmbom and Christofer Sundström, our supervisor respectively examiner at LiU, for their guidance, dedication, and insightful feedback.

Lastly, we would like to thank our friends and family for their smart perspectives and input in how to further develop the model.

Linköping, June 19, 2023
Louise Calmered & Tanja Nyberg

Contents

Abstract iii

Acknowledgments iv

Contents v

List of Figures vii

List of Tables viii

Abbreviations ix

1 Introduction 1
- 1.1 Problem description . . . 1
- 1.2 Aim . . . 2
- 1.3 Research questions . . . 2
- 1.4 Limitations . . . 3
- 1.5 Contributions . . . 3

2 Background and Related Work 4
- 2.1 Background . . . 4
  - 2.1.1 The Swedish National Grid . . . 4
    - 2.1.1.1 Power market: Nord Pool . . . 5
    - 2.1.1.2 Ancillary Services . . . 6
  - 2.1.2 Energy Arbitrage and Peak Shaving . . . 9
  - 2.1.3 Energy Costs . . . 10
  - 2.1.4 Hybrid Energy System . . . 11
  - 2.1.5 Swedish Electric Vehicle Infrastructure . . . 12
- 2.2 Related work . . . 14

3 Modeling Hybrid Energy System 15
- 3.1 Modeling Energy System . . . 15
- 3.2 Battery Energy Storage System . . . 15
- 3.3 Optimization Theory . . . 18
- 3.4 Model Predictive Control . . . 19

4 Design of the Optimization Model 20
- 4.1 Hybrid Energy System Overview . . . 20
- 4.2 Data . . . 22
  - 4.2.1 Warehouse load profile . . . 22
  - 4.2.2 Production from photovoltaics . . . 22
  - 4.2.3 Charging pattern . . . 23
  - 4.2.4 Day-ahead price . . . 24

4.2.5 Frequency Containment Reserve - Disturbance upwards regulation . . 24
4.2.6 Subscription costs . . . 26
4.3 Design of Battery Energy Storage System . . . 27
4.4 Optimization Problem . . . 28
4.4.1 System variables and parameters . . . 28
4.4.2 Objective . . . 29
4.4.3 Constraints . . . 29
4.4.4 Costs . . . 31

5 Result and Evaluation **32**
5.1 Simulation 1.0 - Base Scenario . . . 33
5.2 Simulation 1.1 - Base Scenario . . . 35
5.3 Simulation 1.2 - Base Scenario . . . 37
5.4 Simulation 2.0 - Peak Shaving and Energy Arbitrage . . . 39
5.5 Simulation 3.0 - FCR-D . . . 42
5.6 Simulation 4.0 - Peak Shaving and Energy Arbitrage and FCR-D . . . 45
5.7 Result Summary . . . 48
5.8 Sensitivity Analysis . . . 49
5.8.1 Analysis 1 - Modifying weighting parameters in the objective function . 49
5.8.2 Analysis 2 - Comparing optimal control with predictive control (MPC) . 51
5.8.3 Analysis 3 - Altering day-ahead price and FCR-D remuneration . . . 55

6 Discussion **56**
6.1 Insights and outlook . . . 56
6.2 Method review . . . 58
6.3 Further studies . . . 59

7 Conclusion **60**
7.1 Conclusion . . . 60
7.2 Future work . . . 61

Bibliography **62**

List of Figures

2.1 Volume of bids at FCR-D . . . 7
2.2 Cost of frequency reserves in Sweden between 2016-2025 . . . 8
2.3 Volume increase for different reserves . . . 9
2.4 Electricity cost residential house energy load of 25 000 kWh . . . 11

4.1 Overview of the Hybrid Energy System . . . 21
4.2 Energy load profile year 2022 . . . 22
4.3 PV production pattern year 2022 . . . 23
4.4 Day-ahead price years 2021 and 2022 in SE4 . . . 24
4.5 FCR-D average remuneration years 2021 and 2022 in SE4 . . . 25
4.6 Frequency regulation with stepwise FCR-D activation . . . 25
4.7 BESS internal losses . . . 27

5.1 Result Simulation 1.0 - January . . . 33
5.2 Result Simulation 1.0 - July . . . 33
5.3 Result Simulation 1.1 - January . . . 35
5.4 Result Simulation 1.1 - July . . . 35
5.5 Result Simulation 1.2 - January . . . 37
5.6 Result Simulation 1.2 - July . . . 37
5.7 Result Simulation 2.0 - January . . . 39
5.8 Result Simulation 2.0 - July . . . 40
5.9 Result Simulation 3.0 - January . . . 42
5.10 Result Simulation 3.0 - July . . . 43
5.11 Result Simulation 4.0 - January . . . 45
5.12 Result Simulation 4.0 - July . . . 46
5.13 Analysis 2 - Modifying weighting parameters . . . 50
5.14 Analysis 1 - MPC prediction 5 hours . . . 53
5.15 Analysis 1 - MPC prediction 24 hours . . . 54

List of Tables

2.1 Requirements for ancillary services in Sweden 6
2.2 Charging demand in Stockholm City year 2019 13

4.1 Fast charging pattern over 24 hours 23
4.2 Activation of FCR-D reserves years 2011-2021 26
4.3 Electricity surcharges in price area SE4 in May 2022 26
4.4 Optimization model variables and parameters 28

5.1 Result Simulation 1.0 - Summary year 2022 34
5.2 Result Simulation 1.1 - Summary year 2022 36
5.3 Result Simulation 1.2 - Summary year 2022 38
5.4 Result Simulation 2.0 - Summary year 2022 41
5.5 Result Simulation 3.0 - Summary year 2022 44
5.6 Result Simulation 4.0 - Summary year 2022 47
5.7 Result summary year 2022 - Simulations 1-4 48
5.8 Analysis 1 - Modifying weighting parameters in the objective function 49
5.9 Analysis 2 - Comparison with Model Predictive Control (MPC) 52
5.10 Analysis 3 - Varying day-ahead price and FCR-D remuneration 55

Abbreviations

HES Hybrid Energy System

BESS Battery Energy Storage System

ESS Energy Storage System

EMS Energy Management System

PV Photovoltaics

MPP Maximum Power Point

HEV Hybrid Electric Vehicle

EV Electric Vehicle

VRE Variable Renewable Energy

AC Alternating Current

DC Direct Current

FCR-D up Frequency Containment Reserve - Disturbance upwards regulation

MPC Model Predicitve Control

LV Low-voltage

MV Medium-voltage

HV High-voltage

SoC State of Charge

SoH State of Health

DoD Depth of Discharge

LP Linear Programming

NLP Non-linear Programming

1 Introduction

This chapter introduces the purpose and scope of the entire thesis. Firstly, a description of the problem to be solved is presented. Secondly, the aim of the thesis with the research questions to be answered are given. Lastly, the limitations and contributions are presented at the end of this chapter.

1.1 Problem description

To achieve climate targets and decrease carbon emissions, energy from renewable resources must increase in the energy mix [1], [2]. However, the introduction of renewable resources into the power system elevates the demand for Energy Management Systems (EMS) to maintain a stable power grid and secure frequency stability [3]. The conventional power system is dependent on synchronous generators from hydro- or nuclear power creating mechanical inertia and thereby dampening and decelerating grid fluctuations [4]. Intermittent energy resources are connected to the grid through converters and do not create the same inertia as for the traditional energy resources [4].

Therefore, the combination of stationary batteries or hydrogen storage combined with solar PV or wind has received a great amount of interest in recent years [5]. Combining the electricity production from Battery Energy Storage Systems (BESS) with the use of aggregators, that can pool electricity supply and/or demand and sell this capacity in the electricity markets, could replace the demand for mechanical inertia due to the instant flexibility of batteries. Thus improving the energy security of the power grid and enabling increased electrification.

But there are challenges in delivering renewable energy solutions combined with storage capacity, such as the predictability in variable renewable energy sources (VRE) together with the state of health (SoH) of batteries [1]. Simulation tools are essential to provide reliable results regarding components, and dimensions, and to analyze the impact of different energy solution projects. This can be achieved by analyzing and optimizing the energy flows when installing solar PVs and BESS [6] in a Hybrid Energy System (HES) for example. A HES usually consists of two or more energy systems used in combination to lower the costs, and with better efficiency to ensure the required power output. Installation of HESs has several difficulties, including the fact that it is a common connection point to the grid that limits the amount of energy transferred to and from the grid, along with component boundary

conditions. To simplify investigations and enable further optimization, models are needed to describe and simulate the system.

Models can vary significantly depending on their intended purpose. For most companies, the primary objective is to generate business value and profit. Consequently, the modeling of a HES serves the dual purpose of providing reliable information on system components and dimensions, as well as estimating the system's costs and potential revenues. However, a HES incorporating a BESS can be expensive and may not provide sufficient returns solely through self-consumption generated from the battery, as previous studies have shown [7]. One approach to increase the profitability of a HES is to perform different control techniques such as energy arbitrage or peak shaving, which can lower the overall system cost and result in higher profits [3]. Moreover, by providing supplementary services through the same BESS, such as primary ancillary services like Frequency Containment Reserve - Disturbance (FCR-D), the system can generate additional revenue streams and increase the return on investment. Battery Energy Storage Systems are particularly interesting for frequency control, as it has a fast ramp rate that can help stabilize the frequency in the power grid [7].

While revenues from energy arbitrage, peak shaving, and participation in the frequency containment reserves market have been studied in various cases, the potential profits from combining these strategies have not been thoroughly investigated. In addition, there is a research gap in understanding the behavior and energy flows of a HES when a BESS is optimally utilized in different ways. This gap is particularly evident in larger HESs in Sweden because of its rare existence. Therefore, further research is required to fully explore the benefits and potential of a combined approach to energy arbitrage, peak shaving, and frequency containment reserves, as well as to better understand the optimal use of a BESS in combination with renewable energy in a HES.

1.2 Aim

The project aim is to analyze the energy- and revenue streams in a HES consisting of large-scale PVs, an energy load, a BESS, and with a fast charging station for EVs that also works as an energy load.

A case study is performed for an ongoing installation of a large HES in the south of Sweden, and a model is implemented to analyze different scenarios and optimize the system based on the revenue. Furthermore, suggestions for improvements in technical feasibility and control are made based on sensitivity analyses and simulations.

1.3 Research questions

The research questions evaluated and answered in this project are:

- How can different control techniques of the Hybrid Energy System affect technical feasibility and profitability?
- What is the optimal usage of a Battery Energy Storage System in a Hybrid Energy System considering both revenues and degradability?

1.4 Limitations

The scope is limited to examining the energy flows in HESs with PVs, a BESS, and an energy load based on numbers from an ongoing installation in southern Sweden. Some numbers are modified and not presented in detail in the report due to confidentiality reasons.

The implementation in the model is limited to focusing on modeling the BESS more specifically. The modeling of the PVs and the energy load is limited to input from pre-defined data or assumptions of usage.

Assumptions regarding the demand pattern of the charging station are created from the statistics on the utilization of the charging infrastructure in Sweden together with assumptions in the studied case.

The degradation of the PV park, the charging station, cables, etc is not considered. However, battery degradation is considered because it affects the outcome of different control techniques.

The project focuses on investigating the Swedish ancillary service FCR-D due to it being well-suited to HES with BESS.

Furthermore, this thesis is limited to not discussing the ethical and societal perspectives as though the thesis has been produced in an ethically correct way and followed the general principles of research ethics.

1.5 Contributions

The main strengths of this thesis are listed as contributions below.

- A model for a Hybrid Energy System that can be used to simulate energy cost flows. The system consists of components for load or production that can be varied. The main feature is a BESS which entails the control algorithm and can be seen to serve a bidirectional flow of electricity.
- A methodology to investigate different setups using optimization which adopts energy arbitrage, peak shaving, and battery degradation.
- Ancillary services provide the largest impact on total cost, 500% more revenue per year compared to a system without a BESS. Energy arbitrage and peak shaving provide less impact on the total cost with a smaller increase of 29% in revenue per year.

2 Background and Related Work

This chapter presents relevant research and background to provide enough knowledge for the rest of the thesis. The chapter is divided into two large sections, background, and related work. The background brings up the significant theory of different parts that have to be understood. The section with related work presents similar projects to this thesis to understand what has been done already and where there is a knowledge gap.

2.1 Background

The background section presents the scientific basis with information about the Swedish National Grid, Energy Arbitrage and Peak Load Shaving, Energy Costs, Hybrid Energy Systems (HES), and the Electric Vehicle (EV) Infrastructure in Sweden.

2.1.1 The Swedish National Grid

The Swedish National Grid consists of high-voltage transmission lines and medium- as well as low-voltage distribution lines. The transmission system in Sweden is operated by the national grid operator, Svenska Kraftnät, responsible for ensuring that the electricity supply to the country is secure and stable [8]. The transmission system consists of a 15 000 km high-voltage (HV) network [9], 220 kV or 400 kV transmission lines, that transports electricity from power plants to distribution networks and end-users [10]. These power lines transmit electricity over long distances between regions and countries unlike the distribution lines [9].

The distribution networks, which are owned and operated by regional and local grid operators, deliver electricity to households, businesses, and other consumers. These networks consist of medium and low-voltage power lines of approximately 900 000 km [9] that connect to transformers and substations before reaching the end-users [10]. For the medium-voltage (MV) power lines, the voltage is typically 130 kV but can range from 30-150 kV. The low-voltage (LV) power lines are between 0.4-30 kV [10].

The energy sources supplying electricity to the Swedish energy system can either be connected to the transmission lines or the distribution lines [9]. In Sweden, the energy sources consist of a mix of hydro, nuclear, wind, solar, and thermal power where in 2020, 49% of the electricity generated in Sweden came from renewable energy sources, while the remaining 51% came from nuclear and thermal power plants [9]. The large-scale hydropower and nu-

clear power plants are connected to the transmission network and the smaller-scale wind, solar, bioenergy, and hydropower plants are connected to the distribution network [9].

In order for an energy source to be directly connected to the transmission network, the source has to provide a power capacity of at least 100 MW to the 220 kV lines and 300 MW to the 400 kV lines. However, exceptions of accepting smaller power capacities can be made under certain circumstances [11]. For the energy production connections to the regional grid respectively local grid, the power capacity requirements are 0.1 MW respectively 0.025 MW. In Sweden, approximately 85% of the electricity production is connected to the transmission lines while the remaining 15% is connected to the distribution lines [12]. The number of connections to the distribution grid has increased because of the increase in smaller renewable energy production sources over recent years. For example, the number of grid-connected PV systems increased by 46 % between the years 2020 and 2021. In total, a number of 92 359 PV systems with a total installed power of 1 587 MW were installed in Sweden by the end of 2021 [9].

One of the challenges facing the Swedish power system is the integration of VREs, into the existing infrastructure. There must be a constant balance between the electricity produced and the electricity consumed at all times to keep the frequency constant at 50 Hz which is the standard in the Nordic power grid system [13]. The increase in intermittent energy production together with higher electricity demand, especially during peak hours, has led to difficulties in maintaining the power grid frequency of 50 Hz at all times [14].

2.1.1.1 Power market: Nord Pool

It is Svenska Kraftnät's task to control and monitor Sweden's electrical system around the clock whilst it is the balance responsible party's task to ensure that there is enough power output to meet the energy load in every moment [13]. To do this, the balance responsible parties plan the production based on a forecast of load at every moment together with buying electricity on the power market. Since there always must be a balance between supply and load, the responsible parties will be charged with a balanced settlement afterward if they have delivered too little or too much power compared to the load demand of that hour [13].

Nord Pool is the leading power market in Europe with seven countries included in the Nordic and Baltic market; Sweden, Finland, Denmark, Norway, Estonia, Latvia, and Lithuania. At Nord Pool, there is one day-ahead electricity market called Elspot. At Elspot, producers and consumers make bids before 14:00 for the delivery of electricity for each hour of the next day starting from 00:00 [15]. The other intraday market is called Elbas where the electricity is bought for the current price at latest one hour before the operating hour to adjust for deviating outcomes from bids made on Elspot. The majority of electricity is today traded on Elspot where the day-ahead market stands for almost all the bids and the intraday market only stands for a few percent [15]. Both of the markets on Nord Pool are divided into different bidding areas where Sweden has four different bidding areas with Luleå SE1 in the north all the way down to Malmö SE4 in the south [15]. The price of electricity in each bidding area is determined by supply and demand as well as the transmission capacity between the bidding areas. Since most of the electricity produced in Sweden is produced in the north of Sweden but consumed in the south, the capacity of the power lines to transfer the electricity is decisive for how much electricity that can be delivered and therefore affects the prices [13].

2.1.1.2 Ancillary Services

In most cases, the Nord Pool market can control the balance in the power system and maintain the frequency of 50 Hz by combining Elspot and Elbas. However, in times with a risk of power shortage, there is a requirement for easily activated power reserves to regulate frequency towards 50 Hz [13]. Svenska Kraftnät is the responsible party for this and has a variety of different reserves that can be activated depending on how much the frequency differs. The reserves are procured using bidding on the so-called balance markets, but Svenska Kraftnät can also buy certain reserves on longer contracts [16]. An overview of the categorization and characteristics of the reserves can be found in Table 2.1.

Table 2.1: The characteristics and requirements at the end of the year 2022 of the different reserves in Sweden [16].

	FFR	**FCR-D up**	**FCR-D down**	**FCR-N**	**aFRR**	**mFRR**
Description	Fast Frequency Reserve	Frequency Containment Reserve (Disturbance)	Frequency Containment Reserve (Disturbance)	Frequency Containment Reserve (Normal)	Automatic Frequency Restoration Reserve	Manual Frequency Restoration Reserve
Regulation	Upward	Upward	Downward	Symmetrical up- and downward	Up- and/or downward	Up- and/or downward
Minimum bid volume	0.1 MW	0.1 MW	0.1 MW	0.1 MW	1 MW	10 MW (5 MW in SE4)
Activation (HZ)	Automatically at low levels of rotational energy and frequency changes	49.90-49.50	50.10-50.50	49.90-50.10	Automatically at frequency deviation from 50.00 Hz	Manually at the request of SvK
Activation time	0.7 s (at 49.30 Hz) 1.0 s (at 49.50 Hz) 1.3 s (at 49.70 Hz)	50% within 5 s and 100% within 30 s	50% within 5 s and 100% within 30 s	63% within 60 s and 100% within 3 min	100% within 5 min	100% within 15 min
Endurance	30 s alt. 5 s	$\geqslant$ 20 min	$\geqslant$ 20 min	1 h	1 h	1 h
Volume requirements (Sweden)	100 MW	558 MW	538 MW	231 MW	111 MW	No requirements
Total volume available	115 MW	1 510 MW	955 MW	1 725 MW	1 850 MW	2 100 MW

Table 2.1 shows that the total volume for the different reserves exceeds the average required volume. Consequently, in the balance markets where bids are placed one day in advance, not all bids can be accepted and participate in ancillary services.

Figure 2.1 provides an illustrative example of the daily trading outcomes, showing both the won and lost bids as well as their corresponding prices and volumes. The figure is inspired by an interview with the collaborating energy company.

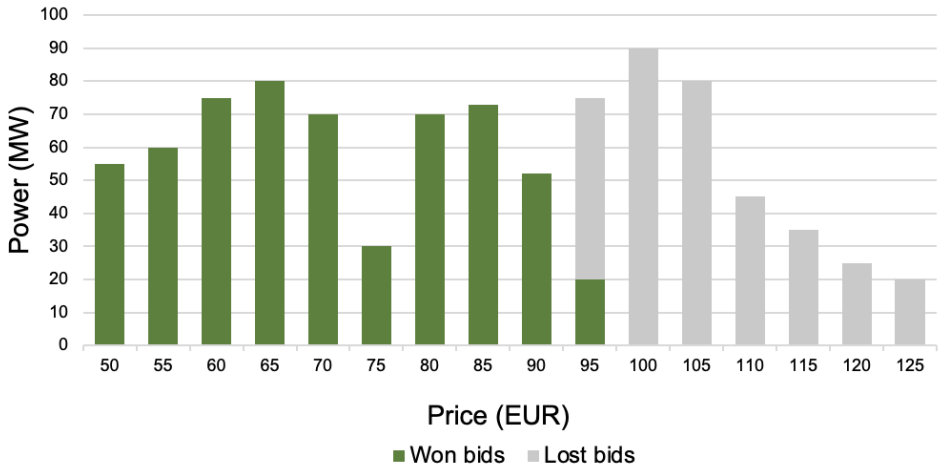

Figure 2.1: An illustrative figure of prices and volume of bids on the daily balance market [1].

One of the reserves to mention further is the Frequency Containment Reserve - Disturbance upwards regulation (FCR-D up) [8]. FCRs are automatically activated if frequency changes occur within a specified frequency range, compared to FRR which can be either automatically or manually activated. FCR is traded one or two days in advance for each second of the day [8]. There are two types of FCR, and FCR-D is one of them. One actor for FCR-D up must be able to deliver a minimum of 0.1 MW to a maximum of 5% of the total bidding volume, which currently is approximately 558 MW, see Table 2.1. The power is linearly activated within the frequency interval of 49.9-49.5 Hz. Additionally, the reserve must be able to deliver 50% of its energy within 5 seconds and 100% within 30 seconds and maintain this flow for at least 20 minutes [8].

According to Svenska Kraftnät [17], a trend towards higher remuneration for ancillary services, particularly FCR-D up, can be observed in Sweden, see Figure 2.2. This is motivating companies' interest in operating in the FCR-D market.

[1] Information obtained from an interview with a company providing EMS in May 2023

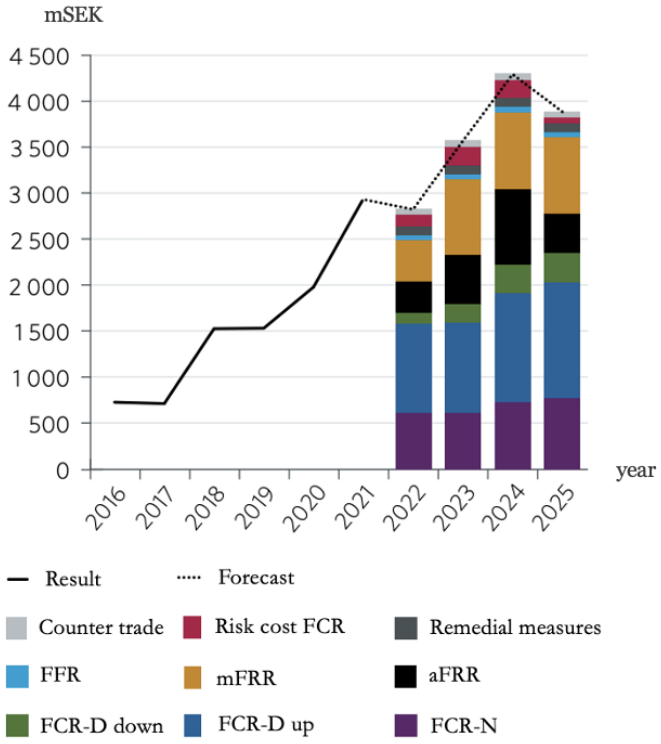

Figure 2.2: The remuneration results for Sweden's different frequency reserves for the last years and the forecast for the upcoming years. For the upcoming years, the remunerations have been divided between different reserves [17].

However, the remuneration for ancillary services has varied across different countries. In the Nordic countries, an analysis of recent historical data shows that the remuneration for FCR-D has experienced an upward trend from 2015 to 2020. Overall in Nordic countries, the highest peak was observed in 2018, and although it remained relatively high in 2019, it experienced a slight decline thereafter [18]. In contrast, Germany has witnessed the opposite trend. The remuneration for FCR-D in Germany has seen a decline, with the average weighted weekly price decreasing from 3 500 €/MWh in 2008 to approximately 1 500 €/MWh in 2019 [19].

Although, increasing remuneration together with the requirements for more power reserves with increasing electricity load, has led to a drastic increase in the total volume of the different reserves over the last few years, see Figure 2.3. Notice the increase in volume for FCR-D down which is a new power reserve that was implemented for the first time in year 2021.

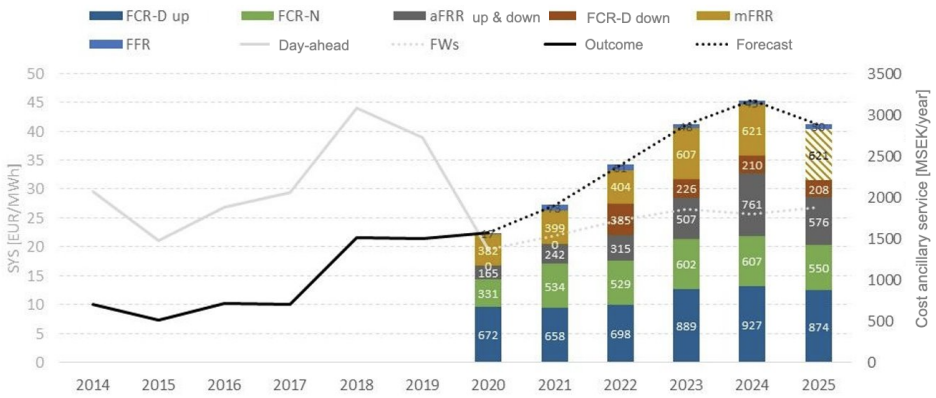

Figure 2.3: Study conducted in 2019 for the expected increase in volume for the different reserves in Sweden [20].

There are several different energy sources that can be adopted in the ancillary services market with BESS being one of them. Frequency regulation is an ideal service to provide for batteries because of their near instantaneous response time [21]. In the FCR provision, the shorter the required full activation time is, the more accurate the response must be with respect to the instantaneous change in frequency. Because of decreasing inertia and increasing share of variable generation, integrating more BESS as fast-responding control reserves is central to supporting power system stability in power systems [22].

Participating in the frequency market would have an impact on battery degradation and the battery's total lifetime. However, FCR-D has been shown to have the lowest response energy turnover. A 1 MW battery completes only about 6 full cycles in the whole year (2018) when participating in the ancillary service market. Due to the very low cycling costs, participating in FCR-D would still generate a profit even though the power price is lower for FCR-D than for FCR-N [22].

According to Wu and Tang [23], the most important BESS requirements for grid frequency regulation service include:

- High power capacity
- Long cycle life at a partial cycle
- Low battery cycle cost
- Fast response

2.1.2 Energy Arbitrage and Peak Shaving

Another strategy to earn money with a BESS, besides ancillary services, is through energy arbitrage. Energy arbitrage means that the actor buys electricity during off-peak hours when the prices are lower and sell it back to the grid during peak hours when the prices are higher. This strategy involves taking advantage of the price difference between off-peak and peak hours to generate profits [24].

One way to utilize energy arbitrage when the customer load profile cannot be scheduled is to implement a BESS. Storage devices such as a BESS can help lower the average electricity prices because it can store produced energy that can be used later, for example storing energy produced during off-peak hours to be consumed during the high peak hours during the day.

That would not only generate a lower cost but also decrease the load of the grid since the system could be self-sufficient. Moreover, it would increase the flexibility in the system which can additionally help handle the challenge of integrating VRE into the electricity system [25].

Energy arbitrage could also be applied in combination with peak shaving to generate even lower costs. The goal for peak shaving is to reduce the power peak in the load profile. The highest power peak an energy load has in a month usually creates an additional cost which will decrease if the power peak decreases, see Section 2.1.3 about costs. Peak shaving can generate multiple benefits such as utilities in generation costs, line loss reduction, and volt support [26]. It can be achieved through different optimization techniques, for example, methods like linear or non-linear and dynamic programming, or heuristic approaches such as particle-swarm optimization [26].

Similarly to participating with the BESS in the ancillary services market, battery degradation also has to be taken into account when investigating energy arbitrage and peak shaving. For a battery system with a C-rate of 1C (e.g. 1C means that the discharge current will discharge the entire battery in 1 hour), a reduction of 12-46% in total revenue due to degradation can be found when the BESS is used for energy arbitrage [18].

2.1.3 Energy Costs

Energy costs for consumers, whether it is private customers or a company, consist of different components outlined in the electricity bill. It requires separate agreements with the electricity trading company for purchasing electricity and the electricity network company for its transportation. The network company holds a local monopoly, limiting choice for the consumer, whereas the trading company can be selected. Typically, the electricity bill is divided into two different invoices, one with the network costs and one with the electricity trading costs, unless both companies are affiliated and provide a combined invoice [27].

The sectioning in the invoices can differ a bit, especially between private customers and companies, but has in general the same structure in Sweden. The electricity trading bill consists of three parts: electricity trading cost, electricity certificate fee, and VAT. The electricity trading cost is linked to the number of kWh used (SEK/kWh) and a fixed monthly subscription cost (SEK/month). The electricity certificate fee also depends on the number of kWh used but is a proportional fee to support renewable energy production. The VAT is lastly added as a percentage of both the electricity trade cost and the electricity certificate fee [27].

In the bill received from the electricity network company, the invoice is usually divided into: the subscription fee, the transfer fee, the energy tax, three additional special fees (often merged as one special fee), and value-added tax (VAT). The subscription fee depends on the size of the fuse which in turn is dependent on the maximum current withdrawn at one moment and is invoiced for the number of days the invoice refers to, usually one month. The transfer fee is the actual transport of electricity in SEK/kWh. The third cost, the energy tax is paid to the network company for them to pay the Swedish Tax Agency and is also represented in SEK/kWh. The three additional special fees are charged for the network monitoring fee, the electricity standby fee, and the electricity security fee. These fees are either paid monthly or yearly and are determined by the Swedish Parliament to transfer further to the Energy Markets Inspectorate, Svenska Kraftnat, and the Swedish Electricity Safety Agency. Lastly, the value-added tax (VAT) in percentage is added here as well [27].

The distribution of energy costs in the electricity bill of a normal size villa heated with electricity and with an energy load of 25 000 kWh can be seen in Figure 2.4.

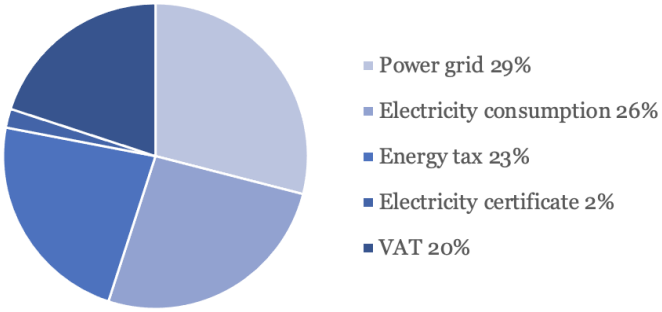

Figure 2.4: The distribution of electricity costs for an electricity-heated normal-size villa with a 20 A fuse and an energy load of 25 000 kWh in Sweden [27].

When an electricity consumer also becomes a producer, the cost parameters change. The revenues from producing electricity depend on several factors, such as whether the production is connected to the distribution or transmission lines, what electricity network company is involved, and the size of the production. Typically, in addition to the subscription for buying electricity, a producer will need a subscription for delivering electricity to the grid. This subscription includes a fixed fee for measuring and reporting the transferred electricity and compensation for the grid costs associated with producing your own electricity. However, in some cases, depending on the fuse size, it may be possible to avoid the fee for measuring and reporting [28].

For larger production sites, above 0.1 MW, the costs and agreement terms are individually designed. In many cases, the revenues from selling electricity back to the grid are based on the day-ahead prices, with a small fee paid to the company responsible for the electricity balance to cover the balance costs [28]. Additionally, a fee of 5-10% is being paid to the company responsible for the control of the frequency regulation when participating in the frequency regulation market.

2.1.4 Hybrid Energy System

There are three main applications of systems containing PV cells: autonomous, hybrid, and grid-connected systems [29]. A HES, usually consists of two or more energy systems used in combination to lower the costs, and with better efficiency to ensure the required power output. For a PV HES, this means a PV generator is combined with a wind turbine or a fuel generator, or both with an Energy Storage System (ESS) [29]. Those HESs are suitable for applications with a continuous demand for high power. The HES can also be connected to the grid using an inverter (DC-AC) [29].

For ESSs, there exist two types which include short-term storage with a storage time of less than 10 min, and long-term storage with a storage time greater than 10 min [29]. What storage system it is can be decided according to mass power, mass energy, number of operating cycles, cost, or energy efficiency. Different types of short-term storage systems are superconductor magnetic energy storage (between 1-10 MW), supercapacitors as charge equalization for a battery or a fuel cell, or flywheel energy storage in EVs. Some long-term storage techniques are pumped hydro energy storage (up to 1000 MW), large-scale compressed air, energy storage in thermal form, or the most common technique; energy storage in chemical form [29].

For a hybrid PV system that is coupled with a BESS, the operating point, which is the intersection of the charge curve and the curve of the PV generator, changes heavily. Therefore, it is of top priority to identify the Maximum Power Point (MPP) to minimize the power

losses of the photo generator [29]. The MPP is used to describe voltage, current, or power for when the system operates at its maximum efficiency [30]. This point is unique for every system and changes continuously because of variations in solar irradiation and temperature throughout the day. To be able to find the MPP, there are different tracking techniques such as the Constant Voltage Method, the Short-Current Pulse Method, or the Open Voltage Method. However, even though the MPP changes, the average MPP can be decided and provided for a certain system in a time-span [30].

2.1.5 Swedish Electric Vehicle Infrastructure

Sweden has been a leader in promoting sustainable transportation, and this includes the development of infrastructure for EVs [31]. According to Elbilsstatistik [32], Sweden had almost 500 000 EVs constituting 9% of all vehicles in Sweden, and 16 000 public charging points for EVs in February 2023, making it one of the countries with the highest density of charging infrastructure per capita. Among these 16,000 charging points, roughly 2 000 are fast charging stations that use direct current (DC) over 22 kW, a number that is increasing as fast charging technology develops. As of now, the maximum output power of a charging station is 350 kW, and there are currently 99 charging points in Sweden capable of delivering this level of power [32]. While charging points capable of delivering high power are mostly utilized for heavy-duty vehicles such as buses and trucks, they have the potential to improve the charging times for light vehicles as well. However, it is important to note that the charging time is not solely dependent on the charging point's output power, but also on the characteristics of the vehicle's battery and its ability to handle high charging currents. This is directly related to the thermal management capabilities of the Battery Electric Vehicle (BEV), which must be considered to ensure safe and effective charging [33].

A report published by the environmental administration of Stockholm City presented findings from a study that analyzed the usage of public charging stations in the city during the year 2019. The study gathered data from 139 000 charging sessions and evaluated approximately 650 normal charging points and 65 fast charging points. Table 2.2 provides a summary of selected results for the most used charging points, which defines the utilization patterns of EVs at both normal and fast charging points [34]. Other studies have found a similar pattern [35].

Table 2.2: General approximate assumptions of the utilization of the most used charging points in Stockholm City from the year 2019 [34].

Assumption	**Normal charging points**	**Fast charging points**
Sessions per day per charging point on weekdays	1.5	4
Sessions per day per charging point on weekends	1.3	2.5
Charge time	2 h	30 min
Energy charged per session	12 kWh	15 kWh
Utilization 11-14 on weekdays	16%	9%
Utilization 9-11 and 14-17 on weekdays	14%	5%
Utilization 17-09 on weekdays	17%	2%
Utilization 12-19 on weekends	13%	5%
Utilization 19-12 on weekends	15%	2%

Compared to gas vehicles, EVs are generally cheaper to operate due to the lower cost of electricity. However, determining the exact cost of charging an EV is challenging as it depends on several factors such as the charging station operator, location, charger type, and the amount of electricity used [36]. In Sweden, fast charging stations are typically more expensive than normal charging stations as they offer a higher charging rate. Below are some rates for the year 2023:

- The rates for OKQ8 are 2.5 SEK/kWh for normal charging while fast charging costs 6.0 SEK/kWh [37].
- The rates for Goteborg Energi are 5.5 SEK/kWh for normal charging while fast charging costs 6.5 SEK/kWh with power below 50 kW, and 8.0 SEK/kWh with power over 50 kW [38].
- The rates for Cirkle K are 5.6 SEK/kW for normal charging while fast charging costs 6.2 SEK/kW with power below 50 kW and 6.9 SEK/kW with power over 50 kW [39].
- The rates for Eon are 6.0 SEK/kW for normal charging while fast charging costs 7.5 SEK/kW with power below 50 kW and 8.5 SEK/kW with over 50 kW [39].

It is worth noting that the cost of charging an EV is subject to change due to market forces, technological advancements, and governmental regulations [36]. The pricing is therefore likely to change a lot over the years and many companies investigate as well as realize dynamic pricing models. Dynamic pricing refers to the practice where the charging provider adjusts the price that end-users pay for charging their vehicles in response to changes in operating conditions. This allows providers to increase charging prices during periods of high electricity prices to better manage the demand for electricity and respond to changes in market conditions [40]. Adopting time-varying pricing can unlock the potential flexibility of EV users which in turn could facilitate the integration of VRE into the power grid [40].

2.2 Related work

There has been a significant amount of research on HESs, including cost reduction and optimal sizing [3, 5, 41]. For instance, a peak shaving case study performed by Möller et al. [3] showed that HES can lead to decreased overall costs. Furthermore, Schreiber et al. [42] implements a model for the optimal design and operation of a HES in Germany for energy arbitrage and automatic frequency restoration reserve applications. The model was developed using Python and solved using the Gurobi framework, with the German balancing market data. The objective of the optimization was to maximize the HES revenue while considering the BESS costs [42].

Ullmark et al. [4] conducted a study that analyzed the demand for inertia and operating reserves in a future carbon-neutral system, and how these services will impact cost-optimized system composition. The study used linear optimization to minimize total HES cost on an hourly basis over a 1-year time horizon [4]. Another study by Jia et al. [43] applied linear programming to investigate a variable charging/discharging method for managing a HES.

According to Xu et al. [44], it is essential to consider the cost of battery degradation when deciding on operating strategies in ancillary services. Previous studies have formulated battery aging models as both linear or quadratic objective functions with respect to active power, energy capacity, and State of Charge (SoC) [45]. Fortenbacher et al. [45] compare degradation for two different battery technologies and found that battery degradation can be substantially reduced by incorporating a battery degradation model. For Hybrid Electric Vehicles (HEVs), 80% of the initial battery capacity remains after 4 000 full cycles.

Li et al. [46] reviews recent advancements in data-driven battery health estimation and discusses their advantages, limitations, and potential next-generation techniques. Harnischmacher et al. [47] perform an analysis in which the results conclude that cycle-count models best represent battery degradation. Furthermore, Xu et al. [44] have also created a counting algorithm to track the number of cycles and incorporate it into the optimization formulation.

In recent years, some studies have focused on optimizing the use of BESSs for both energy arbitrage and ancillary services [48, 7, 49]. Cheng and Powell [49] implement a control strategy for the battery to make charging and discharging decisions at different time scales while accounting for the stochastic information such as load demand, electricity prices, and regulation signals.

Additionally, model predictive control (MPC) is another commonly used approach in EMSs [50, 51, 52]. Sundström et al. [51] use MPC to optimize energy management in smart homes which considers a mathematical model of the household, electric loads, and resources while taking constraints, future information, and predictions into account.

Aguilera-Gonzalez et al. [50] implement an MPC strategy for a grid-connected island with two objectives: maintaining a defined region for power throughput to/from the grid and maximizing the SoC of the BESS while considering the production forecasting data as well as the battery lifespan. The strategy uses the model of the BESS to find the optimal solution that brings the system's predicted output close to a trajectory of future power demand.

This study aims to collect relevant models and strategies from the cited work. To the best of the authors' knowledge, there has been limited research that investigates different control techniques and takes battery degradation into account. Besides, the articles that account for battery degradation do not present the revenue streams from peak shaving compared to operation strategies including ancillary services.

3 Modeling Hybrid Energy System

In this chapter, the theoretical framework from the scientific basis is presented. The chapter displays different alternatives to modeling HES and different optimization techniques. Subsequently in Chapter 4, definitions and notations that form the model for this thesis are presented and motivated.

Since the modeling is limited to focusing on the BESS and the flow between the different components, firstly, general concepts and definitions are described followed by more detailed theory regarding BESS, optimization theory, and MPC.

3.1 Modeling Energy System

In an energy system, the work is the transfer of mechanical energy from one object to another [53]. The energy flow between components can be computed according to Equation (3.1).

$$E = P \cdot t \tag{3.1}$$

Here, energy is denoted by E, power by P, and t is the time.

In a HES, losses such as inverter losses, DC cable losses, AC cable losses, temperature losses, and so on will affect the net energy [53]. Inverter losses are anywhere between 5% and 10% and the inverter is the main source of electric output loss [54], [53]. Both DC cable losses and AC cable losses are between 1% and 3% [54].

3.2 Battery Energy Storage System

Batteries are equipped with an HV battery pack comprising modules and cells arranged in series and parallel configurations. A cell is the smallest unit in the battery and typically has a voltage range of one to six volts [55]. A module consists of multiple cells connected in either series or parallel. Finally, a battery pack is formed by linking modules together in racks in series or parallel configurations [55].

Xavier et al. [54] analyze power converters for BESS connected to MV systems, all topologies presented an efficiency over 94% and some obtained up to 99%.

The energy in a battery can be computed according to Equation (3.2).

$$E = \frac{P}{C_{rate}} \tag{3.2}$$

where P is the power and C_{rate} is the rate at which a battery is discharged relative to its maximum capacity. 1C rate means that the discharge current will discharge the entire battery in 1 hour while 2C means it will discharge twice as fast, in this case discharge fully in 30 minutes [55].

Battery power P at current I, simplified when the inductance is considered negligible, is given by Equation (3.3) [56].

$$P = U \cdot I \tag{3.3}$$

where U is the voltage.

The battery is charged or discharged until it reaches a certain voltage limit [56]. Beyond this limit, the battery cell can sustain irreversible damage to its electrodes. At higher currents, these voltage cutoffs are reached prematurely causing losses due to the increased impact of internal resistance on the cell voltage [56]. These internal losses have to be accounted for when modeling the BESS and are proportional to the square of the current flowing through the battery [57]. The losses are dissipated as heat loss and can be calculated with Equation (3.4).

$$P_{loss} = I^2 \cdot R \tag{3.4}$$

The throughput power can be computed as the internal power added or subtracted by the power losses whether the battery charges or discharges [56], see Equation (3.5).

$$P_{charge} = U \cdot I \pm P_{loss} \tag{3.5}$$

By knowing the power throughput, the battery can be modeled with the state of charge of its battery pack. A method for SoC estimation is Coulomb Counting (CC). CC is an approach that is widely used in SoC estimation due to its simplicity and low computational cost [58]. If P_{charge} is the charging power of the battery and Q_b is the energy capacity of the battery, then the SoC (between 0 and 1) of the battery can be computed according to Equation (3.6). This equation is used for discharging the battery.

$$\frac{dSoC}{dt} = \eta \cdot \frac{P_{discharge}}{Q_b} \tag{3.6}$$

where η is the charging efficiency. The state of health (SoH) can be computed using Equation (3.7).

$$SoH = \frac{Q_{max}}{Q_{rated}} 100\% \tag{3.7}$$

The Q_{max} is the initial maximum charge capacity and the rated charge capacity, Q_{rated} is obtained from calculating the remaining capacity after accounting for the battery degradation. Additionally, battery degradation can be modeled in different ways. Some research includes a degradation cost penalty in the objective function to account for that the battery cannot be cycled an infinite amount of times [59], see Equation (3.8).

$$\arg\min_{P, c_{aging}} \sum_{n_{park}} \sum_{t} \left(P\left(n_{park}, t\right) \cdot p_r(t) \cdot \Delta t + c_{aging}\left(n_{park}, t\right) \right) \tag{3.8}$$

Trippe et al. [59] apply a linear objective function for optimizing HEV charging, where charging power P and battery aging cost c_{aging} are the variables to be optimized. The length of a time step is Δt, and p_r is the electricity price. Additionally, n_{park} and t are indices for the number of the parking events of a car and the time respectively.

Others apply a yearly percentage in terms of degradation depending on lifetime and Depth of Discharge (DoD) and withdraw that percentage from the rated capacity, Q_{rated}. Harnischmacher et al. [47] propose a model for battery degradation that can be defined according to Equation (3.9).

$$Deg\% = \frac{|cd_t|}{CL_{nom} \cdot DoD \cdot 2 \cdot AGV^{cap}} \tag{3.9}$$

where the cd_t is the energy produced by charging or discharging the battery at a time t in kWh, the CL_{nom} accounts for cycle life count under nominal conditions, and the AGV^{cap} correspond to the battery capacity in kWh. The DoD is the amount of charge Q_d removed from the battery at the given state related to the total amount of charge [60], see Equation (3.10).

$$DoD = 100\% \cdot \frac{Q_d}{Q_b} \tag{3.10}$$

In order to account for the battery degradation, the number of cycles the battery adopts has to be calculated. This can be calculated in different ways where Akpinar et al. [61] presents a new battery cycling perspective for energy management of grid-connected BESS and compares it to the rain flow counting method which is the most popular cycling algorithm. The new cycling method is based on the input from a case study of a 2 MW/1 MWh BESS energy management controller's SOC profile. The discharge area, A_n, is calculated in every step and when the cumulative sum of these areas is equal to one full charge/discharge area, that results in one full cycle, see Equation (3.11).

$$A_n = \frac{(SOC_n - SOC_{n-1}) \cdot \Delta t}{2} \tag{3.11}$$

The applied technique in the studied case according to Akpinar et al. [61] recorded a total of 38 cycles over a one-month period for a BESS used for ancillary services. In comparison, when utilizing the rain flow method with SoC values as input data, approximately 600 cycles were observed for SoC levels of 40% and 60%. Unlike the rain flow method, which analyzes variations between values, the method used here involves complete charge-discharge counting at each time step [61]. While originally developed for fatigue materials analysis and stress cycle counting, the rain flow method can be adapted for various applications. Lee et al. [62] outlines the following steps in the rain flow method.

1. Rotate the loading history 90° such that the time axis is vertically downward and the load time history resembles a pagoda roof.
2. Imagine a flow of rain starting at each successive extremum point.
3. Define a loading reversal (half-cycle) by allowing each rainflow to continue to drip down these roofs until:
   a. It falls opposite a larger maximum (or smaller minimum) point.

b. It meets a previous flow falling from above.

c. It falls below the roof.

4. Identify each hysteresis loop (cycle) by pairing up the same counted reversals.

Additionally, the temperature, DoD, or terminal voltage effects can be added to the algorithm with the cost function, both for the new cycle count method and also for the rain flow method to make it more applicable to BESS [61].

3.3 Optimization Theory

Linear Programming (LP) is a mathematical optimization technique that uses linear relationships in the model construction [63]. This method is a preferred choice for modeling interdependencies within energy systems due to its simple approach to optimizing a linear objective function subject to linear equality and inequality constraints [64]. The standard form of an LP algorithm consists of three components: the objective function to be minimized, problem constraints, and non-negative variables [63].

LP has been shown to be particularly useful for decision-making problems with multiple conflicting objectives, as it provides a systematic method for identifying the optimal solution that balances these objectives [65]. In energy systems, LP has been used to optimize energy production, energy transmission and distribution, and energy demand management [66].

Another, a bit more complicated optimization technique is dynamic programming. Dynamic programming is a mathematical optimization method used to solve complex problems by breaking them down into smaller, more manageable sub-problems. It is particularly useful for problems that can be divided into stages, where the optimal decision at each stage depends on decisions made in previous stages [67].

Dynamic programming has been used to optimize the operation of microgrids, EV charging stations, and VRE systems. For example in microgrids, dynamic programming can optimize the dispatch of energy from different sources, such as solar panels and batteries, to meet the energy demand while minimizing the cost and emissions [68].

There are various types of dynamic programming algorithms, such as value iteration, policy iteration, and Q-learning. The choice depends on the specific problem and complexity of the system.

Comparing LP with dynamic programming, LP is a simpler technique that does not take into consideration the effect of time and uncertainty. LP can solve both single-objective functions as well as multi-objective functions but has limitations when it comes to large-scale problems with complex or non-linear situations [69]. A representation of a linear problem is shown in Equation (3.12) where two functions are added, f(x) and g(x), with one of them being multiplied by a transposed vector, λ^T.

$$L(x, \lambda) = f(x) + \lambda^T g(x) \tag{3.12}$$

3.4 Model Predictive Control

For every time step, a Model Predictive Control (MPC) receives or estimates the current state of the system and calculates the control actions that minimize the cost over the chosen time horizon [70]. A constrained optimization problem is then solved depending on the current system state of an implemented model [70]. The controller then applies only the first optimal control action, disregarding the following sequence. In the following time step, the process repeats and new optimal control actions are computed for the prediction time horizon [70]. Aguilera-Gonzalez et al. [50] present a MPC algorithm based on the linear state-space model, see Equation (3.13).

$$\begin{aligned} x(k+1) &= Ax(k) + Bu(k) \\ y(k) &= Cx(k) \end{aligned} \tag{3.13}$$

Here k represents the sampling time x_k is the state vector, u_k is the control input vector, and y_k is the output vector. The predictive methodology is applied by using a state trajectory vector containing estimates for the next N sampling interval i.e the length of the optimization at every k time step.

$$\tilde{x}(k+1) = \begin{pmatrix} x(k+1) \\ x(k+2) \\ \vdots \\ x(k+N) \end{pmatrix}$$

In the same way, the N elements represent the future control sequence contained in the control matrix.

$$\tilde{u}(k+1) = \begin{pmatrix} u(k) \\ \vdots \\ u(k+N-2) \\ u(k+N-1) \end{pmatrix}$$

The output signals containing the variables to optimize are given by $y(k)$.

$$y(k) = [P_{charge}(k) \;\; SoC(k)] \tag{3.14}$$

4 Design of the Optimization Model

Whilst Chapter 3 presents general concepts and theory of modeling HES, this chapter presents the more specific design choices implemented in the model. First, the chapter introduces an overview of the system with its components. Secondly, the data inserted into the model, the optimization problem, and different costs are presented.

The model is implemented in the programming language Python with the package CasADi and the IPOPT solver.

4.1 Hybrid Energy System Overview

The HES being analyzed in the studied case comprises four main components - PV, BESS, Warehouse, and Charging station - in addition to the grid component, which serves as the connection point to the local distribution power grid. The overall system is depicted in Figure 4.1. The model accounts for losses due to rectifiers, inverters, and transformers, as illustrated in the figure. The links in the figure denote the flows between the different components of the HES.

The detailed design of the cables, transformers, converters, and components in the studied case has yet to be determined as it is an ongoing installation. As a result, the authors have made their own assumptions about some of the designs of the system as well as the charging demand. The data of the load and production is however based on real-life data from similar studies or technical data sheets.

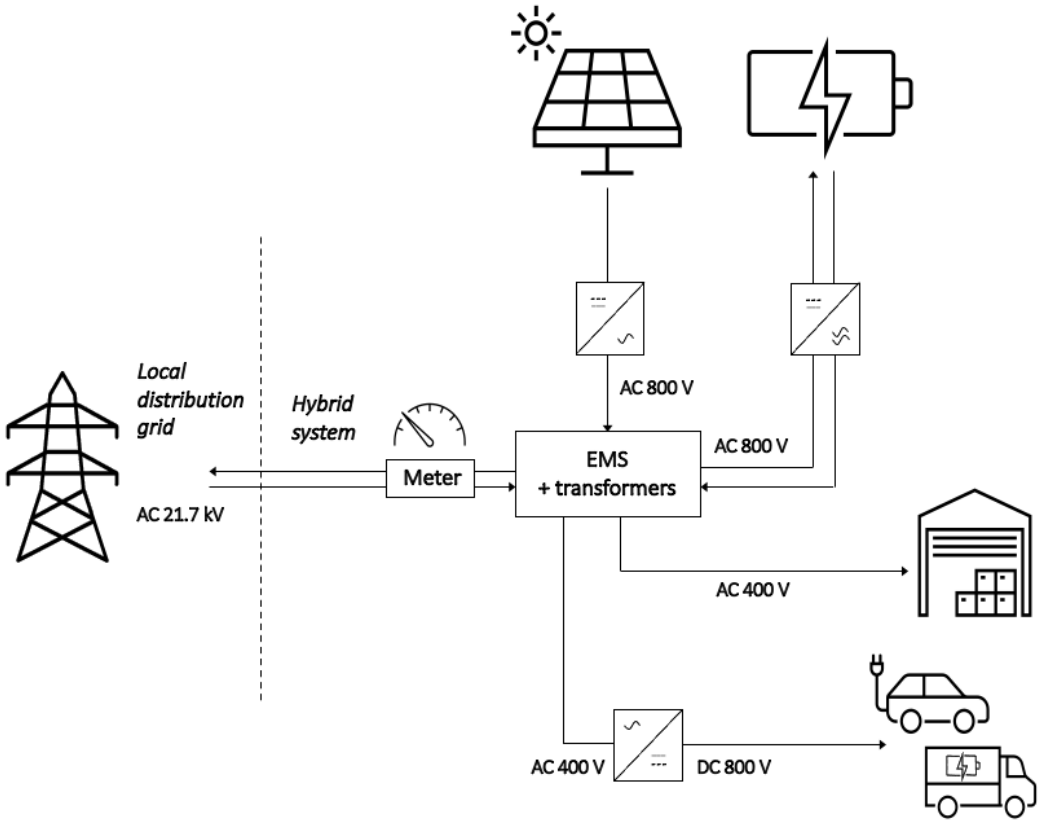

Figure 4.1: A visualization of the components and the flows in the HES model.

The studied system can be seen in Figure 4.1, and is located in the southern region of Sweden in the SE4 electricity tariff area. The hybrid system connection point is connected to a local distribution grid of 22 kV, with a maximum peak power of 2x kW for one hour. The factor x is a scaling factor for the system due to confidentiality reasons and all power and energy sizes are scaled using the same constant. Moreover, it is the same scaling unit for both AC and DC power.

The load of the warehouse has an input at AC 400 V with a known electricity load on an hourly basis. The total energy load for the year 2022 for the warehouse was 720x kWh/year. The proposed charging station has a maximum power output of 2x kW DC. Fast chargers of 350 kW will cover the fast charging needs of electric trucks and private EVs. The station will require a rectifier to convert the 400 V AC from the grid into a DC of 800 V for use in charging.

The PV system requires 10 inverters to convert the DC generated by the panels into AC for integration into the grid with a voltage of 800 V. According to the given simulation data, this PV system is expected to produce approximately 2.2x MWh during one year, with an average output of 0.89x kWh per kWp per year.

The BESS has a capacity of 2x MWh. It is a Lithium Iron Phosphate (LIP) battery and consists of 6 racks of battery strings, each rack as 21 battery packs. The battery packs have 16 cells connected in series. Each string is connected to an individual output of 1 500 V (DC side) and the system requires two converters. One inverter (DC/AC) to discharge and one rectifier (AC/DC) to charge the battery, the AC side is at 800 V entering the transformer.

4.2 Data

The data for the production of the PV system and the load of the warehouse is fixed data obtained from the energy company. This is assembled in vectors with power [W] per hour. The additional load from the fast chargers is based on charging patterns which are explained further in Section 4.2.3.

The model created in Python in the thesis collects data on the day-ahead prices and the FCR-D remuneration from ENTSO-e and Mimer with data for every hour of the years 2021 and 2022. The prices are converted from EUR to SEK with a conversion factor of 10.5 presented in SEK/Wh for the day-ahead price respectively SEK/W for the FCR-D remuneration.

Moreover, the subscription costs are presented, these parameters are manually inserted into the model and are based on the specific case study.

4.2.1 Warehouse load profile

The data is based on data provided by the energy company where the load profile of the warehouse is seen in Figure 4.2(a) and Figure 4.2(b). To the left, the load for the entire year of 2022 is presented, and to the right is the first week of March 2022. The week is chosen due to it being a representative pattern compared to other weeks. The illustration is to show the pattern of load rather than the exact data implemented and because of confidentiality, the exact numbers on the y-axis are erased. Since the plot is adjusted to start on a Monday, notice the higher load on the weekdays compared to the weekends.

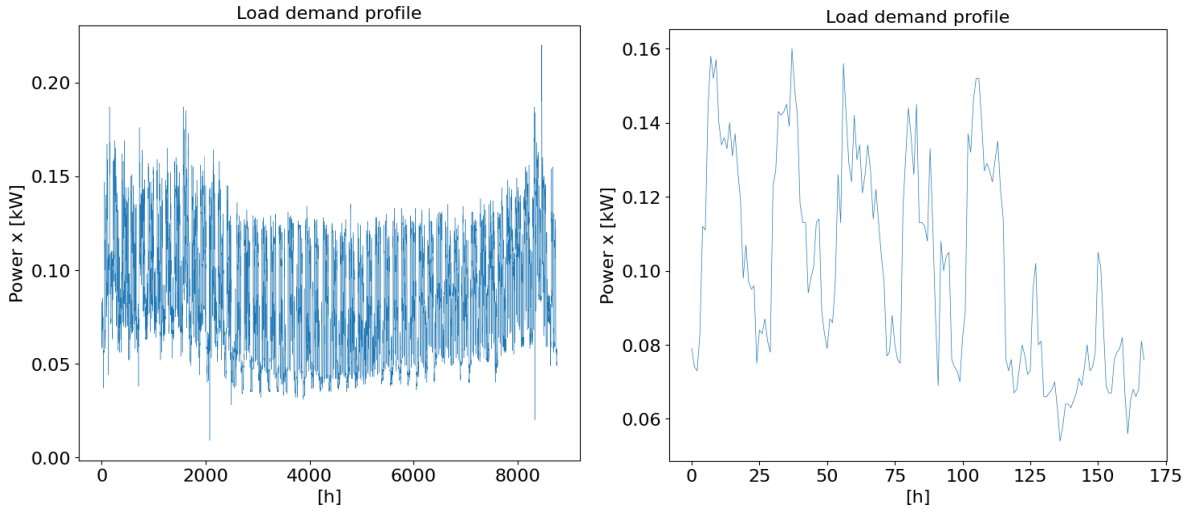

(a) Year 2022

(b) First week of March 2022

Figure 4.2: The energy load demand profile for the year 2022 from January to December in Figure 4.2(a), the first week in March 2022 (adjusted to start on a Monday) in Figure 4.2(b).

4.2.2 Production from photovoltaics

The electricity production from the PV system is based on a case study where the panels are located in the southern part of Sweden. The model uses simulated data for the entire year of 2022, taking into account the actual solar radiation at the location, the number of solar panels, and their technical specifications. Figure 4.3(a) shows the pattern of electricity production from the PV system over the course of an entire year, while Figure 4.3(b) shows

one week in the spring. For confidentiality reasons, the exact amount of electricity produced has been removed, as the case study is based on a real company.

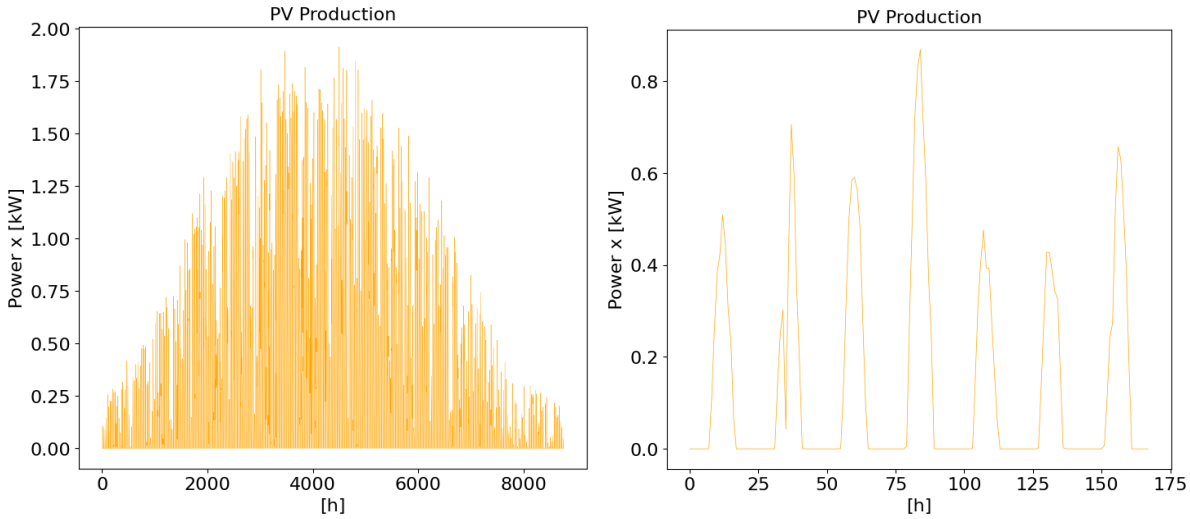

(a) Year 2022

(b) First week of March 2022

Figure 4.3: PV production pattern for the year 2022 from January to December in Figure 4.3(a), a typical diurnal pattern from the first week in March 2022 in Figure 4.3(b).

4.2.3 Charging pattern

Several charging patterns have been examined. The base case charging pattern is based on the general patterns presented in Table 2.2 in Section 2.1.5. Patterns 2023 and 2030 are based on assumptions made by the energy company for those years, which have been modified to represent every hour of the day. The last pattern represents an increasing electrification utilization of fast chargers by the year 2030, based on the assumptions of the base case. Table 4.1 shows the charging patterns for each scenario.

Table 4.1: The energy load of the fast charging station in kWh for different charging patterns over 24 hours.

Hour	00	01	02	03	04	05	06	07	08	09	10	11	12	13	14	15	16	17	18	19	20	21	22	23
Base pattern	15	15	15	15	15	15	15	15	15	30	30	60	60	60	30	30	30	15	15	15	15	15	15	15
Pattern 2023	0	0	8.3	0	0	8.3	0	75	8.3	0	0	8.3	0	0	8.3	75	0	8.3	0	0	8.3	0	8.3	75
Pattern 2030	71	71	71	71	71	71	71	71	71	71	71	71	71	71	71	71	71	71	71	71	71	71	71	71
Base pattern 2030	350	350	350	350	350	350	350	350	350	700	700	1400	1400	1400	700	700	700	350	350	350	350	350	350	350

The model allows for easy switching between these charging patterns, but for the simulations presented in this thesis, only the base pattern has been adopted. Further analysis can be made on how the different charging patterns would impact the results.

4.2.4 Day-ahead price

The hourly day-ahead prices in SEK/kWh for price area SE4 years 2021 and 2022 are presented here. Price area SE4 is chosen due to the location of the HES in the case study. Figure 4.4(a) shows the pattern of the day-ahead price for the entire years 2021 and 2022 to display the variations in day-ahead prices between the different seasons and years.

In Figure 4.4(b), the pattern of the day-ahead price for one week is illustrated to see how peak demand affects the price throughout the day and how it differs between weekdays and weekends. The week visualized is the first week in March 2021 and 2022 starting on a Monday and ending on a Sunday. The week is chosen because it represents a typical pattern and because it is the same week as the patterns in the previous sections.

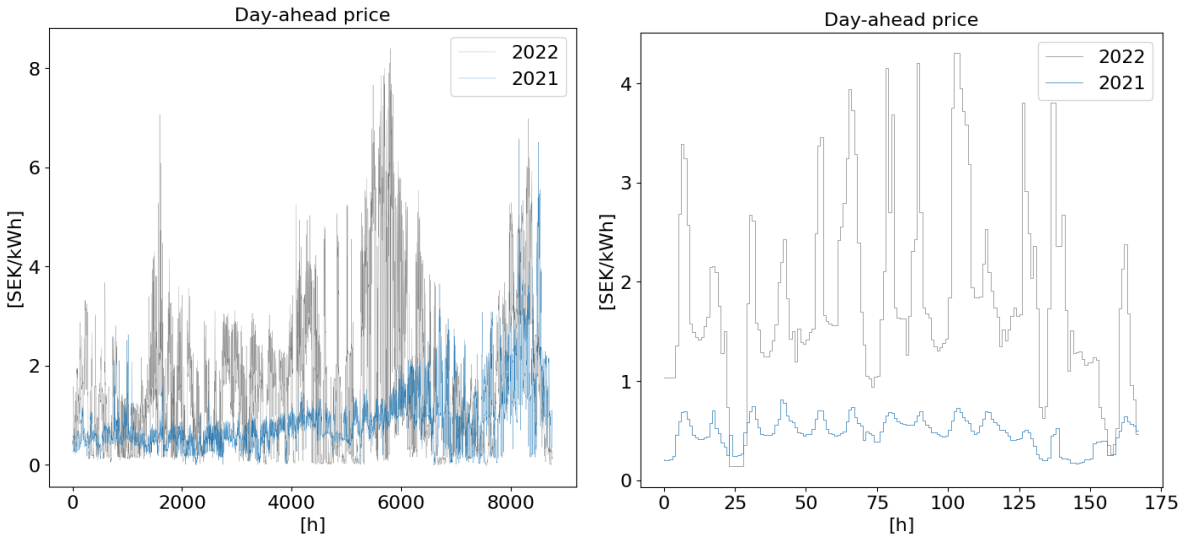

(a) Years 2021 and 2022

(b) First week of March 2021 and 2022

Figure 4.4: The day-ahead prices per hour in SEK/kWh in price area SE4 for the years 2021 and 2022 in Figure 4.4(a), and for the first week of March 2021 and 2022 in Figure 4.4(b) [71].

Comparing the curves from the years 2021 and 2022, the year 2022 is seen to have had much higher day-ahead prices than 2021. This is explained by Russia's invasion of Ukraine as well as the risk of peak demand shortage in Sweden due to less electricity production. Therefore, day-ahead prices from the year 2021 are used in the simulations of this project. Data from a different year can be inserted into the model, however, gap years should be avoided to keep the number of data points constant.

4.2.5 Frequency Containment Reserve - Disturbance upwards regulation

The average hourly remuneration in SEK/kWh for procured FCR-D up across all of Sweden is presented in this section and adopted in the simulations. Also, the probability and total time of activation based on data of the frequency deviations for 10 years are shown stating that the reserve almost never is activated.

The graph in Figure 4.5(a) shows the remuneration of participating in the FCR-D up for the entire years 2021 and 2022 to see the variations between the different seasons and years.

In Figure 4.5(b), the average remuneration for FCR-D up for the first week in March 2021 and 2022 are presented.

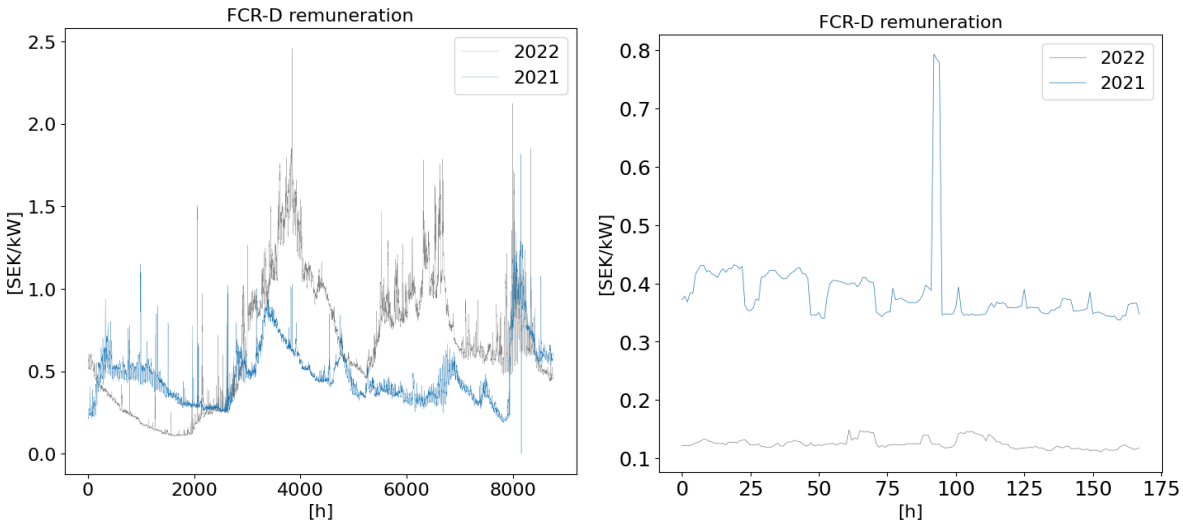

(a) Years 2021 and 2022

(b) First week of March 2021 and 2022

Figure 4.5: The average remuneration in SEK/kW for the entire years 2021 and 2022 respectively for the first week of March 2021 and 2022 [72]

Because of the choice to use data from the year 2021 for the day-ahead prices, data for FCR-D up from the year 2021 will also be adopted in the simulations. However, it should be noticed variations of remuneration throughout the year and differences between the years 2021 and 2022.

The activation of reserves can be monitored by observing frequency deviations in the power grid. Figure 4.6 presents the activation levels of FCR-D at different frequencies, with the grey field indicating the acceptable range of percentage activation at each frequency. When the frequency deviates from 49.90 Hz to 49.80 Hz, 25% of the power reserves that won the bid on the FCR-D market are activated. As the frequency continues to decrease to 49.70 Hz, 50% of the reserves are activated, and so on until the frequency reaches 49.50 Hz.

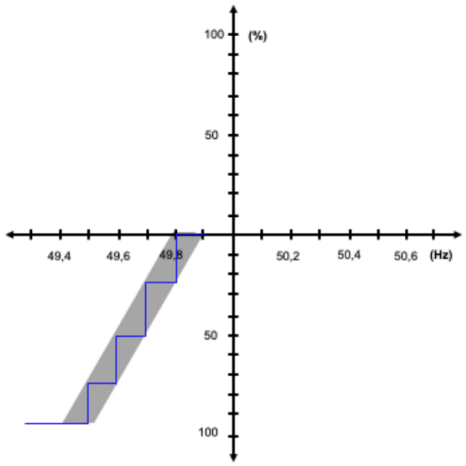

Figure 4.6: Stepwise activation of FCR-D upwards regulation at different frequencies with frequency (Hz) on the X-axis and degree of activation (%) on the y-axis [72].

Table 4.2 is based on data from 2011 to 2021 and shows a consistently low activation time, only around 0.07% requiring activation of 25% when the frequency falls below 49.90 Hz. At 50%, it indicates that all reserves active on the FCR-D market are likely to be activated for only about 2 hours per year.

Table 4.2: Summary of activations of the reserves on the FCR-D market based on data between 2011-01-01 and 2021-03-31. [73].

Frequency, f	Activation	Amount of hours below f	Percentage of hours below f
49.90 Hz	0 %	12 060 h	13.4 %
49.80 Hz	25 %	60 h	0.0668 %
49.70 Hz	50 %	2 h	0.00223 %
49.60 Hz	75 %	0 h	0 %
49.50 Hz	100 %	0 h	0 %

Due to the low activation time, deviation in power will not be modeled in this study. The constraints focus on ensuring that the required power is available in case of activation on the FCR-D upmarket. To simplify the constraints, the bids are assumed to win 50% of cases, see Figure 2.1.

4.2.6 Subscription costs

The subscription costs are based on costs provided by an electricity network company. The numbers for May 2022 are presented in Table 4.3 due to it being the month with all costs available, the day-ahead cost is an approximate number for that month.

Table 4.3: Costs in the electricity bill in the price area SE4 in May 2022. The costs are scaled with the factor of x.

Electricity network			**Electricity trading**		
Electricity transmission	$C_{grid,var}$	0.000075x SEK/kWh	**Day-ahead price**	$C_{dayahead}$	∼0.00155x SEK/kWh
Power grid fee	$C_{P,max}$	0.082x SEK/kW	**Electricity certificate fee**	$C_{trade,cert}$	0.00002x SEK/kWh
Subscription fee	$C_{grid,sub}$	0.5x SEK/mon	**Subscription fee**	$C_{trade,sub}$	0x SEK/mon
Energy tax	$C_{grid,tax}$	0.00036x SEK/kWh	Additional selling fee	$C_{trade,fee}$	0.00003x SEK/kWh
VAT	C_{VAT}	25%	**VAT**	C_{VAT}	25%

The costs are thoroughly explained in Section 2.1.3. The power grid fee is dependent on the maximum power of the month simulated. The subscription fee is dependent on the fuse size of the connection point.

Furthermore, the aggregator (the company responsible for the control) imposes a fee ranging from around 5-20% of the remuneration for participating in the frequency market [1], with 10% being used in this model, $\eta_{fcr,fee}$.

[1] Information obtained from an interview with the collaborating company in April 2023

4.3 Design of Battery Energy Storage System

The modeled BESS is presented in Figure 4.7 showing how the internal losses in the battery affect the power transfer. The power of the battery will be negative if it is being discharged respectively positive when charging. This is further explained in Section 4.4.3.

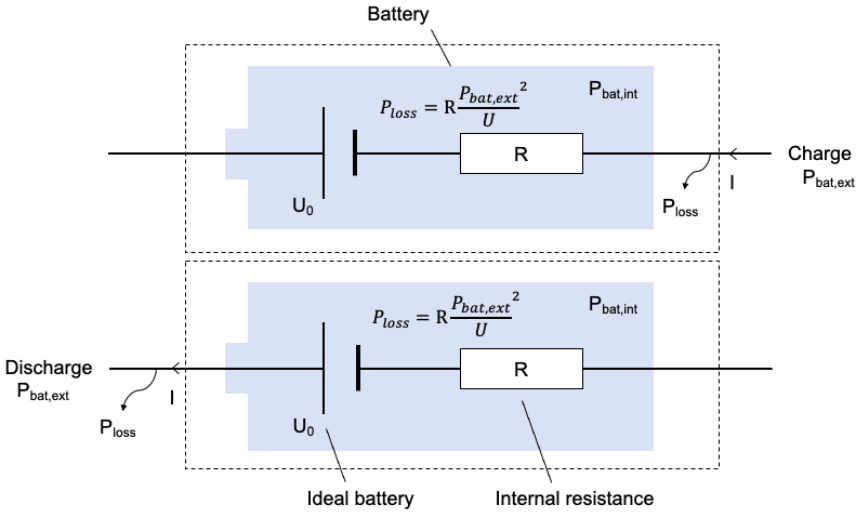

Figure 4.7: Visualization of the BESS with internal losses depending on the throughput power

By reviewing the various battery degradation models implemented from previous research, see Equation (3.7), (3.8), (3.9), (3.10), (3.11), models were compared and the cycle-count method was proven to be the most suitable in this case due to short simulation time and system simplifications. Furthermore, the cycle-count method was also concluded best model representing battery degradation according to Harnischmacher et al. [47] and Akpinar et al. [61].

Therefore, the implemented model includes a calculation according to Equation (4.1) to keep track of the battery's number of cycles in total and on average, where the average should be kept below approximately one full cycle per day [61]. This is to prevent the battery from reaching a high number of cycles (denoted by ψ) to counteract battery degradation. The calculation is performed after optimizing and running the simulation, as it serves as a recommendation rather than a strict constraint to be followed in every iteration. Therefore, the battery can sometimes exceed one full cycle per day if it in the total simulated time has an average of less than one full cycle per day.

$$\begin{aligned} \psi_{full} &= 2 \cdot (SoC_{high} - SoC_{low}) \\ \overline{\psi}_{average,day} &= \frac{\sum_k^N |\Delta \mathrm{SoC_k}|}{\psi_{full}} \qquad k = 0, \ldots, N \end{aligned} \tag{4.1}$$

The first equation calculates the total change in the SoC for one full cycle, where the difference between the upper and lower limits of SoC is calculated. This represents half a cycle, which is why it is multiplied by two to obtain a full cycle.

In the second equation, the average number of cycles per day, $\overline{\psi}_{average,day}$ for the simulation is calculated. The sum of the absolute difference in SoC between every iteration is divided by how much difference in SoC one full cycle is.

4.4 Optimization Problem

The optimization function comprises a main objective, which is divided into three main parts to be minimized, along with several constraints. The system variables and parameters, the main objective, and the constraints are presented in the upcoming subsections.

Once the optimization process has been completed, the costs are calculated and the equations for that are also presented later on in this section.

4.4.1 System variables and parameters

In the model, only vectors (and scalar values) with a predefined length are adopted. The parameters and variables inserted in the model are presented in Table 4.4.

Table 4.4: The name, type, and length of the vectors inserted in the model.

Name	Type	Length	Description
P_{prod}	Parameter	[0...N]	Power produced from PVs every hour
P_{cons}	Parameter	[0...N]	Power load from warehouse every hour
P_{grid}	Variable	[0...N]	Power transferred to/from the grid every hour
P_{bat}	Variable	[0...N]	Power transferred to/from the battery every hour
P_{max}	Variable	[0...M]	The maximum power bought from the grid every month
$C_{dayahead}$	Parameter	[0...N]	The price to buy/sell power from/to the grid every hour
C_{fcr}	Parameter	[0...N]	The remuneration for contributing with reserve capacity every hour
SoC	Variable	[0...N+1]	The internal State of Charge of the battery
ΔSoC	Variable	[0...N+1]	The difference in State of Charge in-between every hour

Parameters are fixed values based on the data gathered presented in section 4.2. The values of the variables are found as the optimization progresses, depending on the constraints set in the formulation. N is the number of hours simulated and M is the number of months simulated.

4.4.2 Objective

The objective function, represented by eq. (4.2), comprises three distinct terms with separate weighting variables. The first term facilitates energy arbitrage, the second term minimizes battery usage to prevent degradation, and the third term focuses on peak shaving.

The selection of weighting variables γ_d, γ_b, γ_p is determined by ensuring that the battery is utilized effectively, avoiding more than one full charge-discharge cycle per day (see Section 3.2 and technical sheets from the case study). γ_d was chosen to a value of 10, γ_b to 1000 and γ_p to 5. Additionally, the chosen values aim to maintain a low P_{max} whilst at the same time allowing for energy arbitrage. The decisions are based on the authors' knowledge when analyzing the resulting graphs presenting the power transfer simulated.

$$\underset{P_{grid},\Delta SoC,P_{max}}{\text{minimize}} \quad \gamma_d \cdot \sum_{k}^{N} P_{grid,k} C_{dayahead,k} + \gamma_b \cdot \sum_{k+1}^{N+1} \Delta \mathrm{SoC_k}^2 + \gamma_p \cdot \sum_{m}^{M} P_{max,k}^2, \qquad k = 0, \ldots, N, \quad m = 0, \ldots, M \tag{4.2}$$

The first term minimizes P_{grid}, and the variable can be positive or negative depending on whether it is more cost-effective to buy or sell power from/to the grid at each hour, $C_{day-ahead}$. The second term with ΔSoC is to maintain a healthy usage of the battery without degrading its lifespan. The third term aims to minimize the maximum peak power every month, P_{max}.

4.4.3 Constraints

The constraints regarding capacity can be found in Equation (4.3). All constraints in the model are bounded by subject to (s.t.).

$$\begin{aligned} \text{s.t.} \quad & P_{low} \leqslant P_{grid} \leqslant P_{high} \\ & P_{low} \leqslant P_{bat} \leqslant P_{high} \\ & SoC_{low} \leqslant SoC \leqslant SoC_{high} \\ & 0 \leqslant P_{max} \leqslant P_{high} \\ & P_{low} \leqslant P_{grid,k} \leqslant P_{max,m} \qquad k = 0, \ldots, N+1, \; m = 0, \ldots, M \end{aligned} \tag{4.3}$$

P_{grid} and P_{bat} are limited by upper and lower limits due to the grid connection point and the battery capacity. The SoC boundaries are set because the battery exhibits a different charging and discharging behavior outside of these limits, for example, due to cut-off voltage.

The lower limit on $Pmax$ is set to zero because the cost for maximum power is only applied to the power transferred from the grid (power bought from the grid). The upper limit, P_{high}, is the maximum allowed peak power in the grid connection point. Each hour, P_{grid} is constrained by the monthly P_{max}.

The battery's SoC is set to have the same start value as the end value to ensure net zero power flow to and from the battery between the start of the simulation and the end of the simulation, see Equation (4.4).

$$\begin{aligned} \text{s.t.} \quad & SoC_{start} = SoC_{init} \\ & SoC_{end} = SoC_{init} \end{aligned} \tag{4.4}$$

The remaining constraints are listed in Equation (4.5) and are applied as constraints for every iteration.

$$\begin{aligned} \text{s.t.} \quad P_{grid,k} &= \begin{cases} P_{bat,ext,k}\eta_c\eta_t - P_{prod,k}\eta_t + \frac{P_{load,k}}{\eta_t}, & \text{if } P_{bat,ext,k} < 0 \\ \frac{P_{bat,ext,k}}{\eta_c\eta_t} - P_{prod,k}\eta_t + \frac{P_{load,k}}{\eta_t} & \text{otherwise} \end{cases} && k = 0, \ldots, N+1 \\ P_{loss,k} &= R\left(\frac{P_{bat,ext,k}}{U}\right)^2 && k = 0, \ldots, N \\ P_{bat,int,k} &= \begin{cases} P_{bat,ext,k}\eta_c\eta_t - P_{loss,k}, & \text{if } P_{bat,ext,k} < 0 \\ \frac{P_{bat,ext,k}}{\eta_c\eta_t} + P_{loss,k} & \text{otherwise} \end{cases} && k = 0, \ldots, N \\ SoC_{k+1} &= SoC_k + \frac{P_{bat,int,k}}{Q_b} && k = 0, \ldots, N+1 \\ \Delta SoC_{k+1} &= SoC_k - SoC_{k+1} && k = 0, \ldots, N+1 \end{aligned} \tag{4.5}$$

Each hourly P_{grid} value is determined by subtracting the battery's charging/discharging power from the combined production of the PV park, load in the warehouse, and fast charging station during that specific hour. The efficiency factors take into account whether the battery is being charged or discharged.

The next constraint accounts for the losses in the battery which are calculated according to the third constraint where U is the battery's voltage and R is the internal resistance, see Figure 4.7.

The subsequent SoC value is calculated based on the previous value of the SoC, adjusted by the charging or discharging power of the battery. Further details on this model used to calculate the SoC can be found in Section 3.2.

4.4.4 Costs

The costs considered include variable costs, fixed costs, charging revenues, revenues from the FCR-D upmarket, and costs for maximum power output from the grid each month.

$$\sum_{k}^{N} C_{var,k} = \begin{cases} \sum_{k}^{N} P_{grid,k} \cdot \left(C_{dayahead,k} + C_{grid,var} + C_{grid,tax} + C_{trade,cert} \right), & \text{if } P_{grid,k} > 0 \\ \sum_{k}^{N} P_{grid,k} \cdot \left(C_{dayahead,k} - C_{trade,fee} \right) & \text{otherwise} \end{cases} \qquad k = 0, \ldots, N$$

$$\sum_{m}^{M} C_{fixed,m} = \sum_{m}^{M} C_{grid,sub,m} + C_{trade,sub,m} \qquad m = 0, \ldots, M$$

$$\sum_{k}^{N} C_{char,k} = \sum_{k}^{N} P_{char,k} \cdot C_{char} \qquad k = 0, \ldots, N$$

$$\sum_{k}^{N} C_{fcr,k} = \sum_{k}^{N} (Q_{fcr} \cdot \eta_{acc,bid}) \cdot (C_{fcr,k} \cdot \eta_{fcr,fee}) \qquad k = 0, \ldots, N$$

$$\sum_{m}^{M} C_{P,max,m} = \sum_{m}^{M} P_{max,m} \cdot C_{P,max} \qquad m = 0, \ldots, M$$

(4.6)

$C_{var,k}$ is the variable cost which includes the day-ahead price, grid transmission cost, energy tax, and electricity certificate fee. When buying electricity and when selling electricity it is the day-ahead price, subtracting a fee charged by the trading company. $C_{fixed,m}$ are two monthly subscription costs charged by the trading company and the electricity grid company. $C_{char,k}$ is the revenue from the fast charging station. $C_{fcr,k}$ is the revenue for every hour for the average reserve capacity, withdrawing a percentage of a fee paid to the company responsible for the control of the EMS. This is in turn multiplied by the average accepted bids. Lastly, the cost for the maximum power $C_{p,max,m}$ bought from the grid every month is calculated.

The total costs for the time simulated can be calculated through Equation (4.7).

$$C_{tot} = \sum_{k}^{N} C_{var,k} + \sum_{m}^{M} C_{fixed,m} - \sum_{k}^{N} C_{char,k} - \sum_{k}^{N} C_{fcr,k} + \sum_{m}^{M} C_{P,max,m} \qquad k = 0, \ldots, N, \;\; m = 0, \ldots, M$$

(4.7)

The charging costs and the costs of participating in the FCR-D up are subtracted whilst the others are added. C_{fixed} and $C_{P,max}$ are monthly costs instead of hourly costs. C_{tot} is lastly multiplied by the value-added tax (VAT) based on its positive or negative nature. A positive value, a cost, is multiplied by 100% plus the VAT (1.25 using the numbers in Section 4.2.6). A negative value, a revenue, is multiplied by 100% minus the VAT (0.75 based on Section 4.2.6).

5 Result and Evaluation

The different simulations are described, presented, and summarized in this chapter. The simulations are:

- Simulation 1.0 - Base Scenario: Energy load profile
- Simulation 1.1 - Base Scenario: Energy load profile + PV production
- Simulation 1.2 - Base Scenario: Energy load profile including fast chargers + PV production
- Simulation 2.0 - Peak Shaving and Energy Arbitrage: Energy load profile including fast chargers + PV production + Optimal control algorithm for energy arbitrage and peak shaving
- Simulation 3.0 - Participation with ancillary service FCR-D upwards regulation: Energy load profile including fast chargers + PV production + Market participation for FCR-D with a BESS
- Simulation 4.0 - Peak Shaving and Energy Arbitrage and FCR-D: Energy load profile including fast chargers + PV production + Optimal control algorithm for energy arbitrage and peak shaving + Market participation for FCR-D with a BESS

All simulations have inputs according to the data described in Chapter 4.2. The parameters and variables used are described in Chapter 4.4. The output in the simulations is the required amount of bought or sold energy, P_{grid} over a set range of time, and control signals such as SoC for the battery or the $C_{dayahead}$ (see Section 4.2.4), and different costs and revenues. The simulations are performed for one year. The tables presenting the results in costs and energy are scaled according to a factor x. Positive numbers imply a cost and negative numbers stands for revenues. The total costs of every simulation are compared and analyzed in Section 5.7.

5.1 Simulation 1.0 - Base Scenario

Simulation 1.0 is modeled with the energy load profile solely to represent a system without PV or battery installation. In Figure 5.1 and Figure 5.2 the results from the first week of January 2022 and July 2022 are presented.

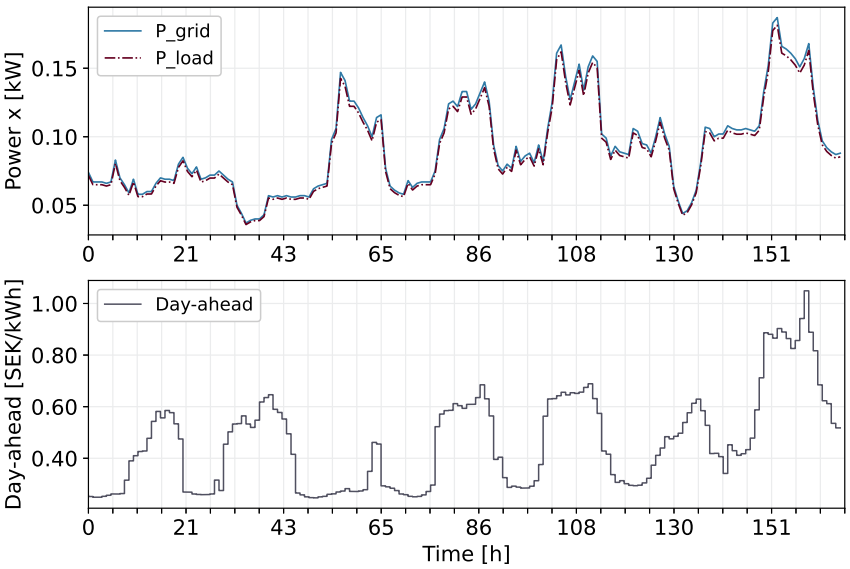

Figure 5.1: Energy bought from the grid the first week in January 2022

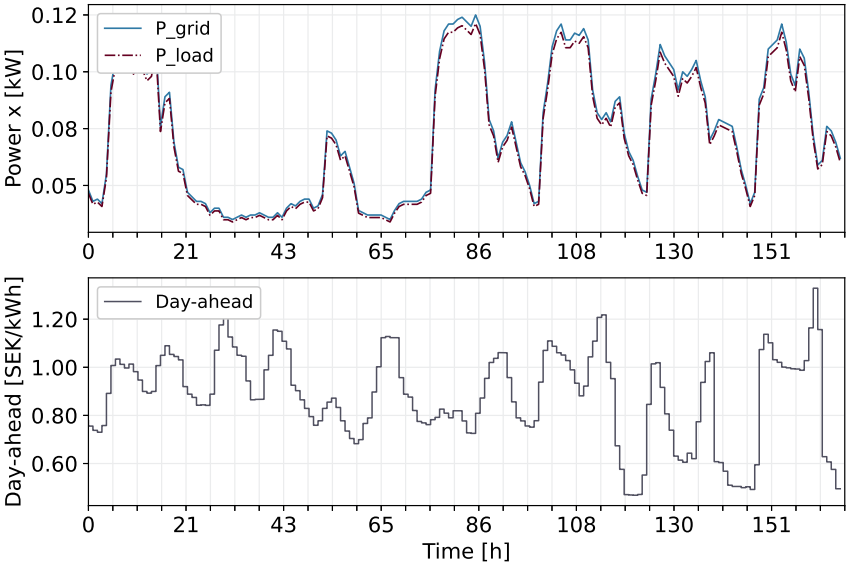

Figure 5.2: Energy bought from the grid the first week in July 2022

Figure 5.1 show that the bought electricity from the grid is a bit higher than the load to account for transmission losses. The figure also shows the same pattern as Figure 4.2(b) that the power demand is higher on the five weekdays and lower during the weekend (the graphs are starting from t=0 which is Friday 00:00).

Figure 5.2 show the same pattern that Figure 5.1 does but with a lower amount of power needed. In Table 5.1, the total different monthly costs for an entire year are presented. The column to the far right presents the sum of all other costs, including VAT, resulting in a total cost for the HES. The total amount of electricity transferred between the grid and the hybrid energy system together with the maximum power peak is also displayed in the table.

Table 5.1: The different costs per unit x for an entire year from the first simulation 1.0 with an energy load are presented for every month and in total.

	P_max [kW]	**E_mon [kWh]**	**C_var [SEK]**	**C_fix [SEK]**	**C_p,max [SEK]**	**C_charg [SEK]**	**C_fcr [SEK]**	**C_tot [SEK]**
January	0.187x	71.2x	71x	0.5x	15x	0x	0x	108x
February	0.165x	67.6x	71x	0.5x	14x	0x	0x	106x
March	0.187x	73.9x	70x	0.5x	15x	0x	0x	107x
April	0.158x	56.7x	51x	0.5x	13x	0x	0x	81x
May	0.131x	53.0x	52x	0.5x	11x	0x	0x	79x
June	0.134x	53.8x	66x	0.5x	11x	0x	0x	97x
July	0.135x	52.2x	62x	0.5x	11x	0x	0x	92x
August	0.133x	56.4x	76x	0.5x	11x	0x	0x	110x
September	0.135x	58.1x	102x	0.5x	11x	0x	0x	142x
October	0.138x	62.2x	90x	0.5x	11x	0x	0x	127x
November	0.155x	70.4x	122x	0.5x	13x	0x	0x	169x
December	0.220x	78.0x	196x	0.5x	18x	0x	0x	269x
Total:	**Max: 220x**	**754 000x**	**1 029x**	**6x**	**154x**	**0x**	**0x**	**1 487x**

In the table, the fixed cost are seen to be the same every month. The maximum power delivered from the grid varies a bit but results in a pretty similar power peak cost anyway. The total cost varies the most monthly due to the difference in variable costs which is based on how much electricity is being bought every month. The electricity load is higher during the winter months and lower during the summer, most probably because of the need for more heating in the winter.

5.2 Simulation 1.1 - Base Scenario

Simulation 1.1 has the same input data as Simulation 1.0 but with PV production added to represent customers with already existing PV production. The results of the simulation for the first week of January 2022 and July 2022 are shown in Figure 5.3 and Figure 5.4 respectively.

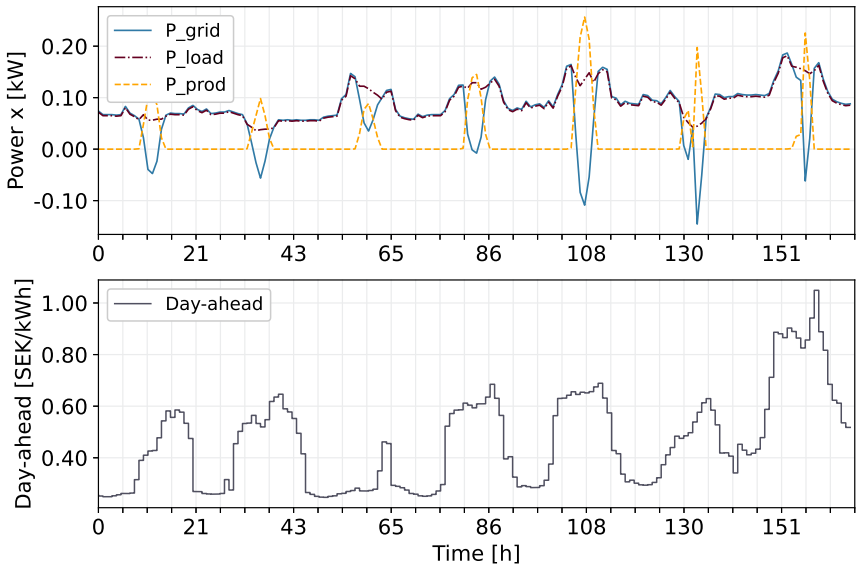

Figure 5.3: Power transferred to/from the grid every hour the first week in January 2022 including production from PVs.

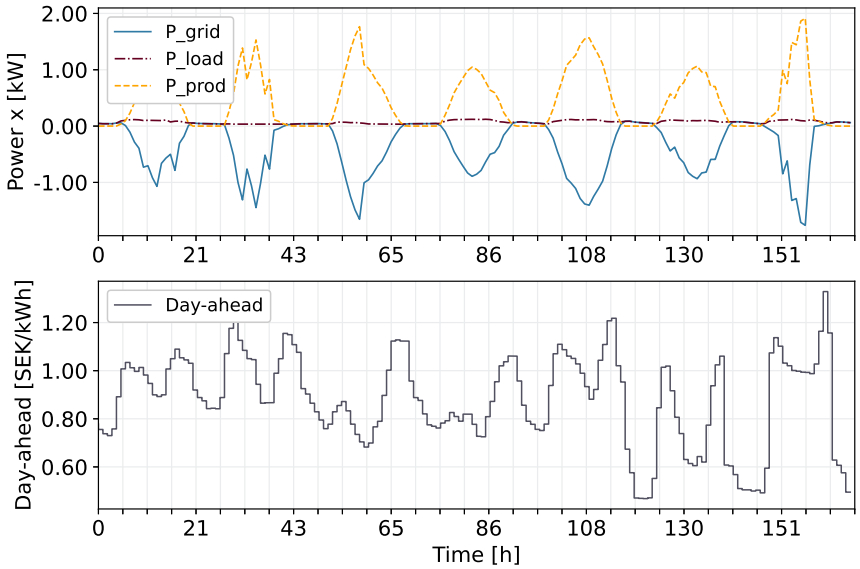

Figure 5.4: Power transferred to/from the grid every hour the first week in July 2022 including production from PVs.

In the top graph in Figure 5.3, during the night, when there is no production from the PVs, the graph is the same as in Simulation 1.0 where the electricity bought from the grid is almost the same as the load. The transmission losses η_t are almost even out because in order to account for the load, a bit more power is needed, but the production has some losses which result in a bit less power sold back to the grid. During the day, the electricity is sold to the grid due to the production from the PVs after adjusting for the load.

In Figure 5.4, the PV panels generate significantly more electricity, resulting in a higher amount of energy sold to the grid. The scale on the y-axis of the graph is noticeably different from that of the winter week, reflecting the much larger production during the summer. This indicates that such high levels of production can result in substantial savings in energy costs. The results presented in Table 5.2 provide support for this claim.

Table 5.2: The different costs per unit x for an entire year from simulation 1.1 with an energy load plus production from PVs are presented for every month and in total.

	P_max [kW]	**E_tot [kWh]**	**C_var [SEK]**	**C_fix [SEK]**	**C_p,max [SEK]**	**C_charg [SEK]**	**C_fcr [SEK]**	**C_tot [SEK]**
January	0.181x	45.0x	49x	0.5x	15x	0x	0x	80x
February	0.171x	6.3x	28x	0.5x	14x	0x	0x	53x
March	0.157x	-89.9x	-17x	0.5x	13x	0x	0x	-3x
April	0.135x	-192.7x	-75x	0.5x	11x	0x	0x	-48x
May	0.107x	-291.9x	-136x	0.5x	9x	0x	0x	-95x
June	0.095x	-305.7x	-216x	0.5x	8x	0x	0x	-156x
July	0.102x	-298.3x	-214x	0.5x	8x	0x	0x	-154x
August	0.084x	-221.1x	-178x	0.5x	7x	0x	0x	-128x
September	0.092x	-122.8x	-138x	0.5x	8x	0x	0x	-97x
October	0.118x	-27.2x	-29x	0.5x	10x	0x	0x	-14x
November	0.125x	38.9x	72x	0.5x	10x	0x	0x	104x
December	0.145x	62.7x	155x	0.5x	12x	0x	0x	209x
Total:	**Max: 181x**	**-1 396 700x**	**-699x**	**6x**	**124x**	**0x**	**0x**	**-248x**

Table 5.2 displays the results of Simulation 1.1 with PV production, demonstrating a significant increase in the monthly energy transfer between the grid and the system, particularly during the summer months. It can be concluded that the PV park exceeds the load by a considerable amount, resulting in revenues for eight out of twelve months. Although the power peak varies each month, it remains relatively low, and the costs associated with it are insignificant compared to the variable costs, which account for most of the variation in the total costs each month.

5.3 Simulation 1.2 - Base Scenario

Figure 5.5 and Figure 5.6 displays the resulting output and control signals for the third base scenario with energy load including a charging station and PVs for the first week of January 2022 and July 2022.

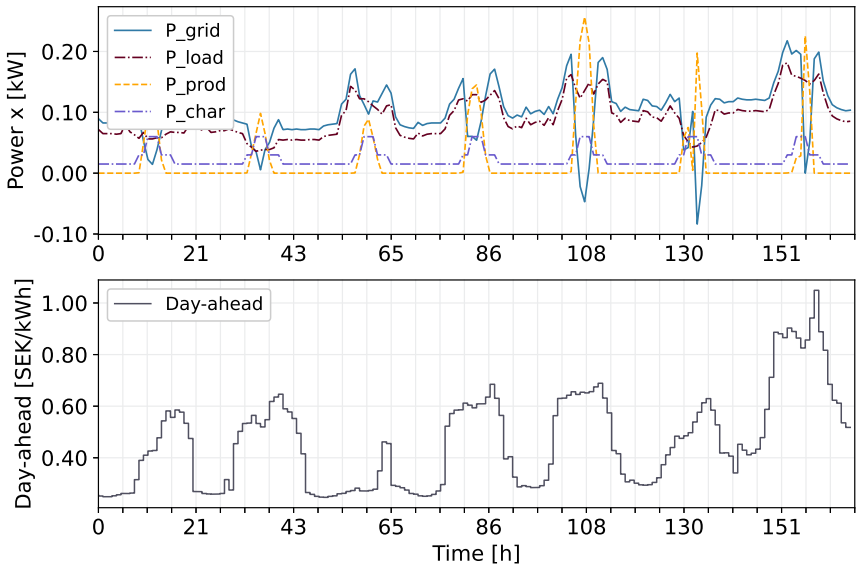

Figure 5.5: Power transferred to/from the grid every hour the first week in January 2022 including production from PVs and extra load from the charging station.

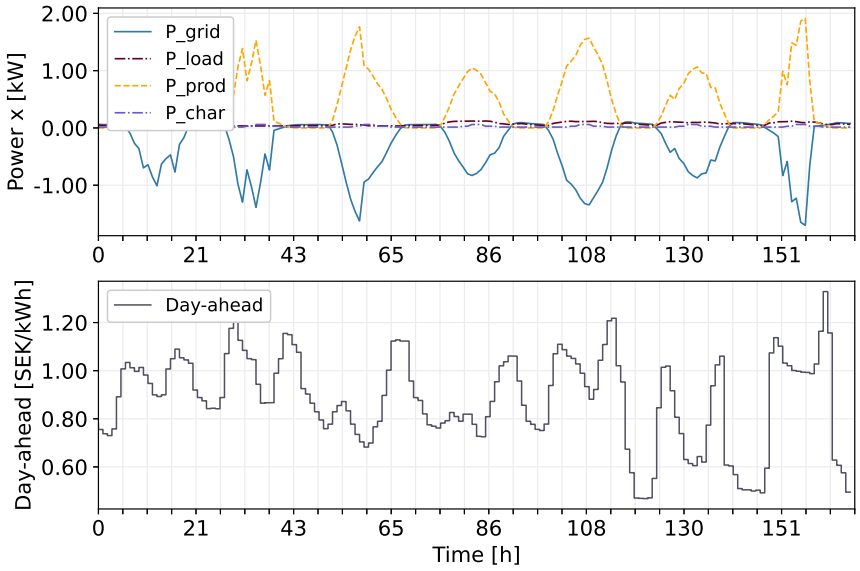

Figure 5.6: Power transferred to/from the grid every hour the first week in July 2022 including production from PVs and extra load from the charging station.

Figure 5.5 shows a higher total load P_{load} and P_{char} than for the previous Simulation 1.1 and Figure 5.3. Therefore, not as much electricity P_{grid} is sold back to the grid when the solar production P_{prod} reaches high peaks.P_{char} is seen to have a higher load during the day, according to Table 4.1 with the different charging patterns, for the simulations, pattern 1 was used.

Figure 5.6 shows a similar pattern to Figure 5.4 but with a slightly higher energy load due to the extra demand from the charging station. The resulting costs for the base scenario adding an extra load in the form of fast chargers are presented in Table 5.3.

Table 5.3: The different costs per unit x for an entire year from simulation 1.2 with an energy load including fast charging plus production from PVs are presented for every month and in total.

	P_max [kW]	**E_mon [kWh]**	**C_var [SEK]**	**C_fix [SEK]**	**C_p,max [SEK]**	**C_charg [SEK]**	**C_fcr [SEK]**	**C_tot [SEK]**
January	0.211x	62.6x	64x	0.5x	15x	-53x	0x	34x
February	0.186x	22.3x	41x	0.5x	14x	-48x	0x	10x
March	0.172x	-72.2x	-6x	0.5x	12x	-53x	0x	-35x
April	0.150x	-175.6x	-66x	0.5x	10x	-51x	0x	-80x
May	0.122x	-274.2x	-125x	0.5x	9x	-53x	0x	-126x
June	0.110x	-288.6x	-202x	0.5x	10x	-51x	0x	-182x
July	0.117x	-280.7x	-199x	0.5x	8x	-53x	0x	-183x
August	0.099x	-203.4x	-161x	0.5x	9x	-53x	0x	-154x
September	0.107x	-105.7x	-114x	0.5x	11x	-51x	0x	-115x
October	0.133x	-9.5x	-8x	0.5x	13x	-53x	0x	-36x
November	0.155x	56.0x	100x	0.5x	15x	-51x	0x	80x
December	0.243x	80.3x	199x	0.5x	20x	-53x	0x	208x
Total:	**Max: 243x**	**-1 188 700x**	**-476x**	**6x**	**146x**	**-624x**	**0x**	**-579x**

In Table 5.3, what stands out are the monthly revenues from the fast charging station. Comparing these revenues to the other costs in the Table, they are seen to be fairly large for the first and last months of the year resulting in a smaller cost in total for these months. During the summer months, the revenues from fast chargers are much smaller in comparison to the revenues from selling produced energy back to the grid. Additionally, Simulation 1.2 requires more power due to an extra energy load resulting in both a higher maximum power every month as well as more energy delivered from the grid every month. However, the costs for this do not affect the total costs as much as the revenues from the fast chargers.

5.4 Simulation 2.0 - Peak Shaving and Energy Arbitrage

In Simulation 2.0 a BESS is implemented with control for peak shaving and energy arbitrage. In Figure 5.7 and Figure 5.8, the first week in January 2022 and July 2022 is presented.

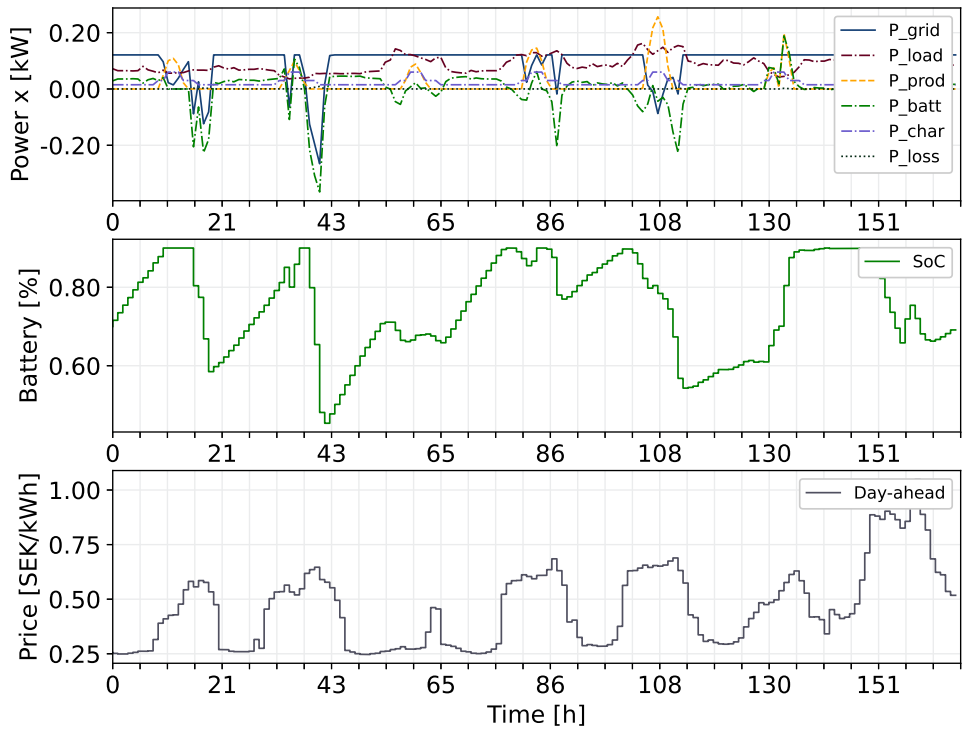

Figure 5.7: Peak shaving and energy arbitrage scenario for the first week in January 2022 with PV and charging.

From Figure 5.7 it is displayed that the battery can in cases of high load work as an extra source of power to minimize the maximum power peak transferred from the grid, which further minimizes the cost. It can also shift the energy load profile throughout the day depending on the day-ahead price, adopting energy arbitrage. When the battery curve in the top graph, $P_{battery}$, is below zero, it means the battery is being discharged. It is seen that the battery is being used when the load is high and the day-ahead price (in the bottom graph) is high. This is seen in the middle graph showing the variations in the battery's SoC. As a result, it allows the electricity bought from the grid, P_{grid}, to be kept at a constant level almost all the time. Therefore, it minimizes the power peaks which in turn decreases the cost.

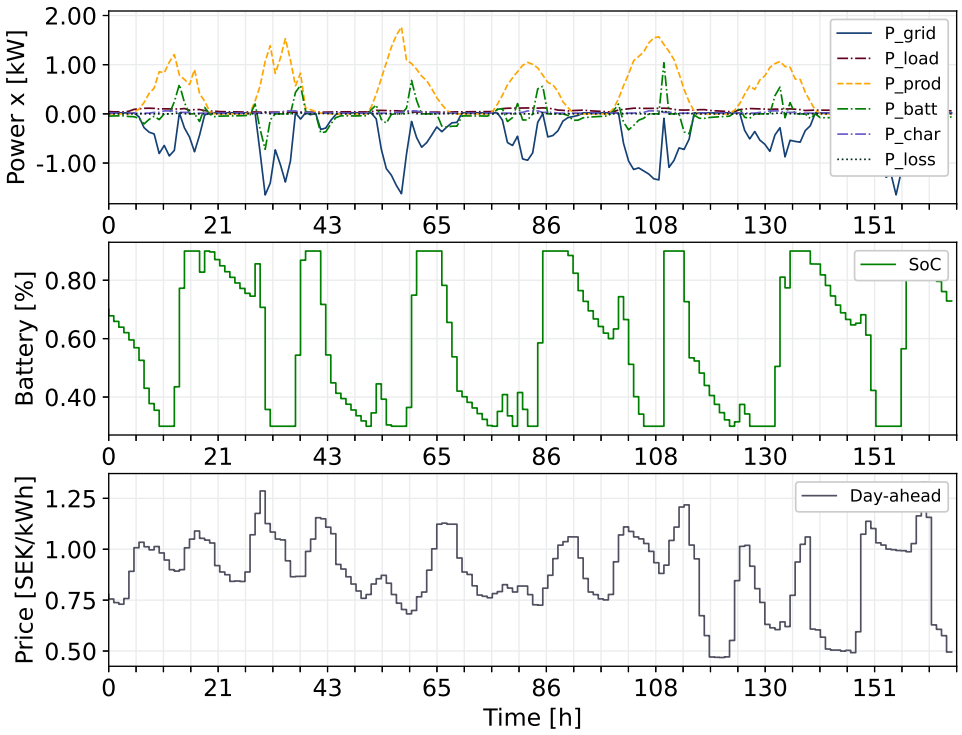

Figure 5.8: Peak shaving and energy arbitrage scenario for the first week in July 2022 with PV and charging.

As the production from the PV system is much higher in the summer compared to the winter, a different pattern is observed in Figure 5.8. In this graph, P_{grid} covers the consumption, however, since the production is very high, the system is almost self-sufficient. It should be noted that the scale on the graph is different due to the much higher production, which reaches above 0.825x a few times, compared to Figure 5.7 where the production is a maximum of 0.115x. Due to this higher production, the battery can be charged and discharged more frequently during the day, which explains the behavior observed in the middle graph. This results in a higher number of cycles in the summer compared to the winter. However, the total number of battery cycles in a year is 338 cycles, with an average of approximately 0.93 cycles per day, which is lower than 1 to ensure that the battery does not degrade too much over time.

In Table 5.4, the monthly different costs are presented for Simulation 2.0. Also, the power transferred from the grid as well as the maximum power per month is shown. The yearly total is displayed at the bottom of the table.

Table 5.4: The different costs per unit x for an entire year from Simulation 2.0 with peak shaving and energy arbitrage are presented for every month and in total.

	P_max [kW]	E_mon [kWh]	C_var [SEK]	C_fix [SEK]	C_p,max [SEK]	C_charg [SEK]	C_fcr [SEK]	C_tot [SEK]
January	0.109x	66.6x	65x	0.5x	9x	-53x	0x	27x
February	0.095x	27.8x	36x	0.5x	8x	-48x	0x	-5x
March	0.047x	-65.5x	-19x	0.5x	4x	-53x	0x	-51x
April	0.032x	-167.0x	-78x	0.5x	3x	-51x	0x	-95x
May	0.009x	-262.2x	-136x	0.5x	0.8x	-53x	0x	-141x
June	0.007x	-276.6x	-210x	0.5x	0.6x	-51x	0x	-195x
July	0.027x	-269.2x	-203x	0.5x	2x	-53x	0x	-190x
August	0.019x	-193.3x	-170x	0.5x	2x	-53x	0x	-166x
September	0.058x	-99.0x	-128x	0.5x	5x	-51x	0x	-130x
October	0.065x	-3.9x	-20x	0.5x	5x	-53x	0x	-50x
November	0.116x	60.0x	96x	0.5x	10x	-51x	0x	68x
December	0.148x	83.8x	185x	0.5x	12x	-53x	0x	181x
Total:	**Max: 148x**	**-1 099 300x**	**-584x**	**6x**	**60x**	**-624x**	**0x**	**-747x**

In Table 5.4, only January, November and December have in total a cost for buying electricity. All the other months have a negative number on the total costs showing that because of the production and use of the BESS, the power sold back to the grid override the costs of buying electricity resulting in revenue instead of cost for that month. The maximum power output each month is relatively low and has decreased compared to Simulations 1.0 and 1.1 which results in a decrease in the maximum power cost each month. In this simulation, the fast charging station is included in the system accounting for a significant income because of selling electricity to the consumers charging their EVs. This together with the decrease in maximum power output also affects the amount of electricity transferred between the grid and the system and results in a smaller amount sold in the summer and a larger amount bought in the winter compared to Simulation 1.1. The variable costs therefore increase in the winter and the revenues decrease in the summer.

5.5 Simulation 3.0 - FCR-D

In Simulation 3.0, the participation with ancillary services, more exactly with the frequency containment reserve FCR-D upwards, is simulated. The amount of electricity in the BESS is kept on the same level at all times where the SoC is approximately 70% to be able to deliver the amount of power being procured in case of activation. This accounts for approximately 1x over 20 minutes when the percentage of accepted bids is assumed to be around 50%. As explained previously, the actual activation is not implemented and shown in this thesis due to the low activation time of the year. The result simulated is the result of revenues from participating in the FCR-D upwards market with the battery's entire capacity.

The participation in FCR-D upwards market of the first week in January 2022 is presented in Figure 5.9.

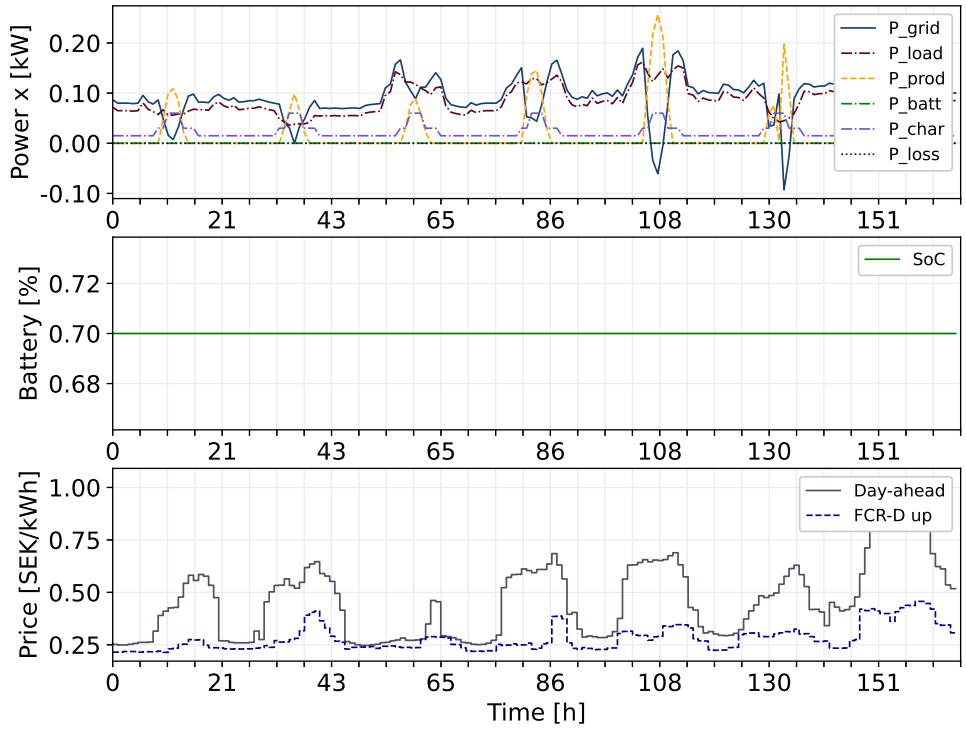

Figure 5.9: FCR-D scenario for the first week in January 2022 with PV and charging.

The top graph in the figure presents the same pattern as Simulation 1.2. The middle graph shows the constant SoC at approximately 70%.

In the bottom graph, both the day-ahead price and the FCR-D upwards remuneration are plotted. The FCR-D upwards remuneration can be seen to be much lower than the day-ahead price. However, the FCR-D upwards remuneration provides only revenues and no costs in contrast to the day-ahead price that also stands for a cost whenever electricity has to be bought from the power grid. This together with the large capacity of the BESS participating with ancillary services compared to the actual amount of power that can be sold back to the grid every hour will result in much larger revenues from the remuneration of the FCR-D upwards market than from selling on the day-ahead market.

The same scenario with FCR-D but for the first week of July 2022 is presented in Figure 5.10.

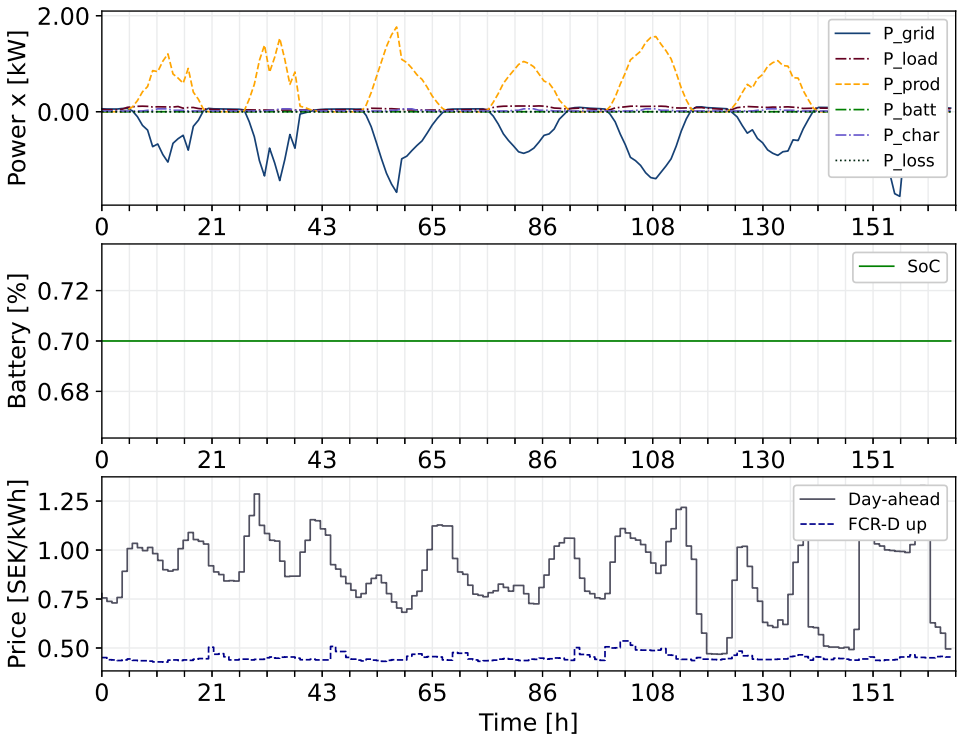

Figure 5.10: FCR-D scenario for the first week in July 2022 with PV and charging.

The thing worth noticing in this graph is the bottom graph where the FCR-D upwards remuneration is very low compared to the day-ahead price. The day-ahead price also has a lot more variations throughout the week shown. However, the FCR-D upwards remuneration is generating approximately the same amount of revenues in the summer as in the winter. This is confirmed by the monthly costs presented in Table 5.5.

Table 5.5: The different costs scaled with x for an entire year divided into monthly costs from the Simulation 3.0 presenting a HES with a BESS participating in the FCR-D up market.

	P_max [kW]	E_mon [kWh]	C_var [SEK]	C_fix [SEK]	C_p,max [SEK]	C_charg [SEK]	C_fcr [SEK]	C_tot [SEK]
January	0.211x	62.6x	64x	0.5x	17x	-53x	-316x	-215x
February	0.170x	22.3x	41x	0.5x	14x	-48x	-308x	-225x
March	0.172x	-72.2x	-6x	0.5x	14x	-53x	-223x	-201x
April	0.124x	-175.6x	-66x	0.5x	10x	-51x	-223x	-247x
May	0.116x	-274.2x	-125x	0.5x	10x	-53x	-448x	-462x
June	0.117x	-288.6x	-202x	0.5x	10x	-51x	-377x	-465x
July	0.100x	-280.7x	-199x	0.5x	8x	-53x	-325x	-426x
August	0.107x	-203.4x	-161x	0.5x	9x	-53x	-257x	-347x
September	0.133x	-105.7x	-114x	0.5x	11x	-51x	-221x	-281x
October	0.155x	-9.5x	-8x	0.5x	13x	-53x	-283x	-248x
November	0.185x	56.0x	100x	0.5x	15x	-51x	-223x	-119x
December	0.243x	80.3x	199x	0.5x	20x	-53x	-511x	-258x
Total:	**Max: 243x**	**-1 188 700x**	**-476x**	**6x**	**150x**	**-624x**	**-3 714x**	**-3 493x**

The table shows a significantly higher total revenue compared to the previous scenarios, primarily due to the revenues generated from the FCR-D upwards market. When compared to Simulation 2.0, which involves energy arbitrage and peak shaving, the total amount of power sold to the grid during a year is roughly the same in both scenarios and for every month. However, the maximum power generated over the year and each month is significantly higher in the FCR-D scenario without peak shaving and energy arbitrage, resulting in a higher cost. Nevertheless, the revenues from the FCR-D market every month are much higher than the cost, making it a profitable scenario overall. The profits from fast charging and the fixed costs are the same as in Simulation 2.0.

5.6 Simulation 4.0 - Peak Shaving and Energy Arbitrage and FCR-D

The final scenario combines the results of Simulation 2.0, which focused on peak shaving and energy arbitrage, with Simulation 3.0, which involved participating in the FCR-D upwards market. The simulation model imposes a lower limit on the BESSs SoC of approximately 60% to ensure that it remains active on the FCR-D upwards market, while simultaneously utilizing the remaining capacity for peak shaving and energy arbitrage.

Simulation 4.0 for the first week in January 2022 is presented in Figure 5.11.

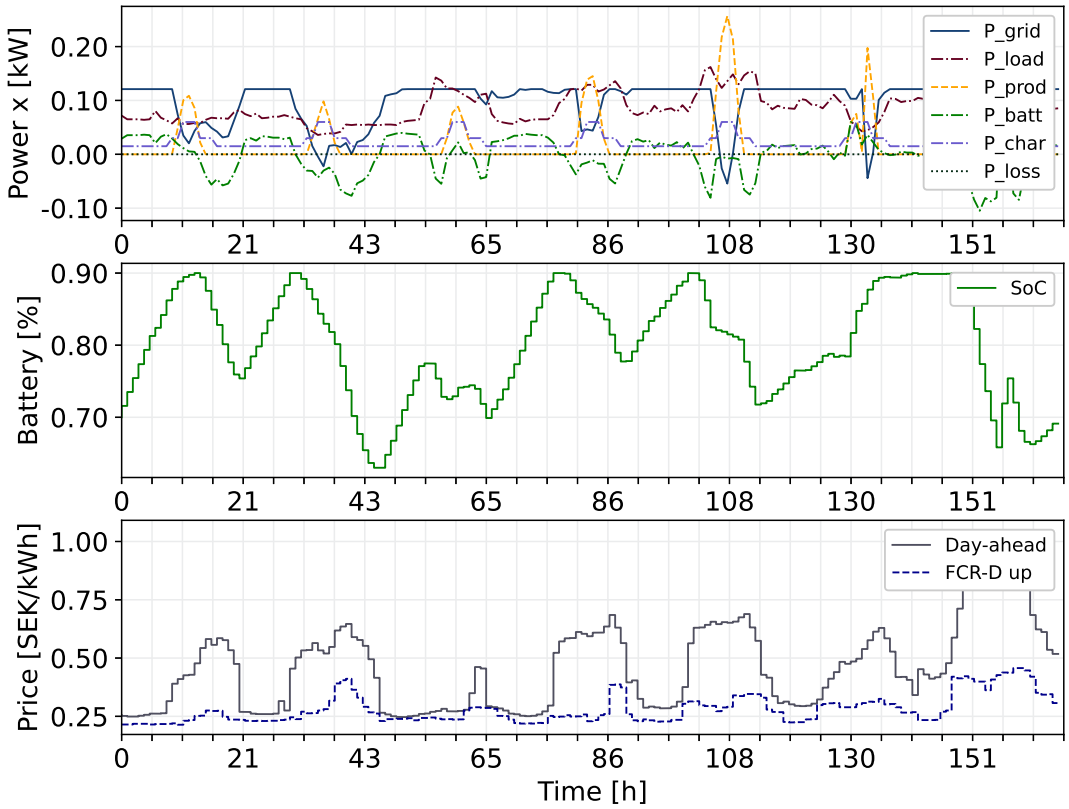

Figure 5.11: Peak shaving and energy arbitrage and FCR-D scenario for the first week in January 2022 with PV and charging.

The battery, P_{batt}, in the top graph in the figure is not active as much as in Simulation 2.0 with only peak shaving and energy arbitrage but can still be seen to be adopted for peak shaving and energy arbitrage, just on a smaller scale. The electricity bought from the grid is pretty constant, except for during the day with a larger PV production. The middle graph shows how the SoC varies between approximately 0.6 and 0.9 to still have enough power to deliver in case of activation on the FCR-D market. The total number of full cycles for this simulation is 125 which provides an average of 0.34 cycles per day. This is very few cycles resulting in a low degradation of the battery. It can be explained due to one full cycle still being between the upper and lower accepted limits of SoC for the battery, and not the lower limit for the battery in this specific case.

A week in the middle of the summer, the first week in July 2022, is presented in Figure 5.12.

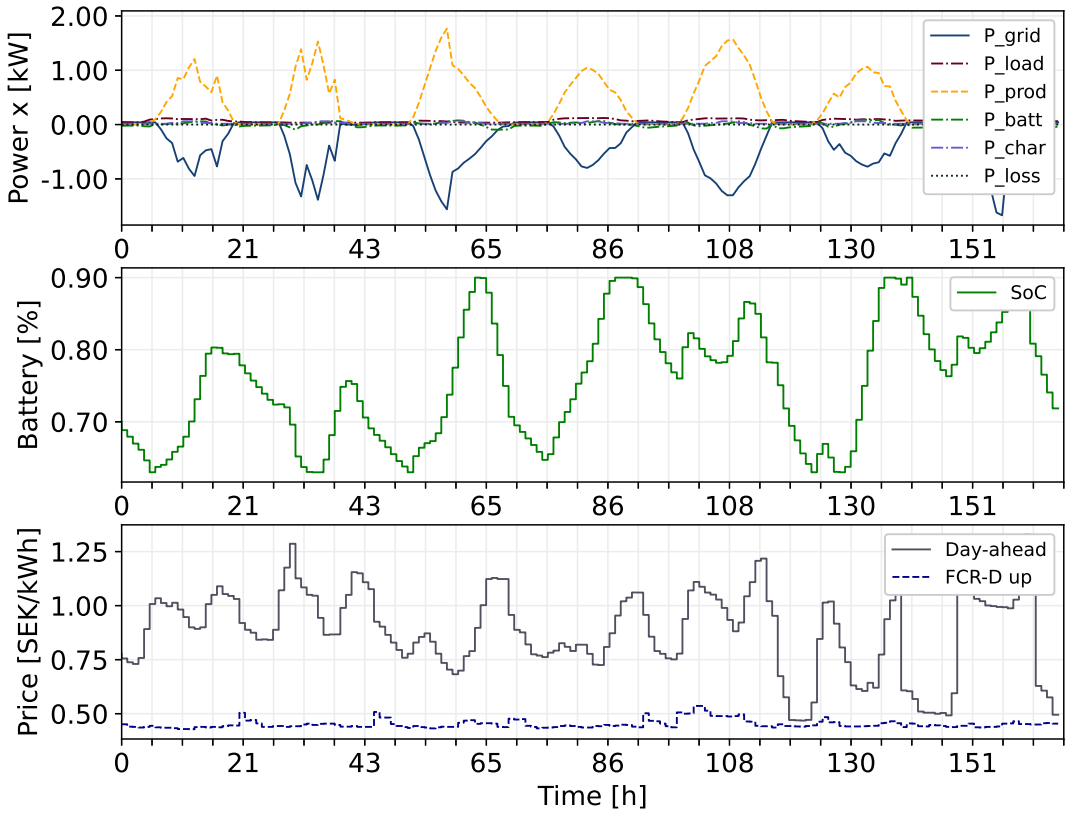

Figure 5.12: Peak shaving, energy arbitrage, and FCR-D scenario for the first week in July 2022 with PV and charging.

The first week of July exhibits significantly higher electricity production, resulting in less variation in the battery's capacity as evident from the graph. However, the middle graph still displays a similar range of SoC fluctuations, with SoC varying between 0.6 and 0.9, as observed during the first week of January.

The total costs and energy transferred to/from the grid from Simulation 4.0 are shown in Table 5.6.

Table 5.6: The different costs per unit x for an entire year is divided into monthly costs from the simulation presenting a HES with a BESS participating in the FCR-D up market and with peak shaving.

	P_max [kW]	E_mon [kWh]	C_var [SEK]	C_fix [SEK]	C_p,max [SEK]	C_charg [SEK]	C_fcr [SEK]	C_tot [SEK]
January	0.118x	66.3x	65x	0.5x	10x	-53x	-316x	-220x
February	0.110x	26.7x	38x	0.5x	9x	-48x	-308x	-231x
March	0.091x	-64.9x	-8x	0.5x	7x	-53x	-223x	-207x
April	0.057x	-166.0x	-68x	0.5x	5x	-51x	-223x	-253x
May	0.036x	-261.6x	-125x	0.5x	3x	-53x	-448x	-467x
June	0.033x	-275.8x	-199x	0.5x	3x	-51x	-377x	-468x
July	0.048x	-267.9x	-194x	0.5x	4x	-53x	-325x	-425x
August	0.050x	-193.0x	-159x	0.5x	4x	-53x	-258x	-349x
September	0.069x	-98.3x	-114x	0.5x	6x	-51x	-221x	-285x
October	0.082x	-4.3x	-13x	0.5x	7x	-53x	-283x	-256x
November	0.126x	59.8x	95x	0.5x	10x	-51x	-223x	-126x
December	0.179x	83.4x	181x	0.5x	15x	-53x	-511x	-276x
Total:	**Max: 179x**	**-1 095 600x**	**-501x**	**6x**	**82x**	**-624x**	**-3 714x**	**-3 563x**

All the months of the year generate revenues for the variable costs because of selling electricity to the grid instead of buying, except for January, February, November, and December. The value of $C_{P,max}$ is low for all months, lower than for Simulation 3.0 with only FCR-D upwards. This is of course because of the penalty of P_{max} to reduce peak power and make use of energy arbitrage (the last term in the optimization equation presented in Section 4.4.2). The result is a bit higher total revenue for each month compared to the FCR-D scenario. C_{charg} and C_{fixed} are the same as for the other scenarios due to the same load of fast chargers, the same fixed cost for every month, and the same length of the simulation.

5.7 Result Summary

This chapter presents a summary of the previously presented scenarios. Table 5.7 displays the costs, the total energy transferred between the grid and the system as well as the maximum power bought from the grid during the entire year. Moreover, the difference in the percentage of the total costs between the four last scenarios is shown.

Table 5.7: Result summary of yearly revenue stream for the different scenarios per unit x. C_{fixed} is the same for all scenarios and is therefore not presented in the table.

	P_max [kW]	E_mon [kWh]	C_var [SEK]	C_p,max [SEK]	C_charg [SEK]	C_fcr [SEK]	C_tot [SEK]	Diff_Ctot [%]
1.0	0.220x	754.0x	1 029x	155x	0x	0x	1 487x	+356%
1.1	0.181x	-1 397x	-699x	124x	0x	0x	-248x	+57%
1.2	0.243x	-1 189x	-476x	146x	-624x	0x	-579x	0
2.0	0.148x	-1 099x	-584x	60x	-624x	0x	-747x	−29%
3.0	0.243x	-1 189x	-476x	150x	-624x	-3 714x	-3 493x	−503%
4.0	0.179x	-1 096x	-501x	82x	-624x	-3 714x	-3 563x	−515%

From Table 5.7 it is displayed that Simulation 1.0 with an energy load is the only simulation that obtained a yearly total energy cost. By installing PVs as in Simulation 1.1, the system will produce more energy than the internal load and thereby obtain revenue from excess sold electricity. Simulation 1.2 shows a higher total revenue compared to Simulation 1.1 which is due to the extra profit from the charging stations. However, the variable costs for Simulation 1.2 result in less revenue than the variable costs for Simulation 1.1. The reason for this can be explained by a smaller amount of electricity sold back to the grid due to the extra load of fast chargers introduced in the simulation. By installing a BESS in Simulation 2.0, the variable cost C_{var} generates more revenue compared to Simulation 1.2 which shows that the optimization adopts energy arbitrage more than in Simulation 1.2. Simulation 2.0 also decreases the maximum power bought from the grid, P_{max} due to the peak shaving adopted.

Comparing the total costs between all the simulated scenarios, the remuneration from FCR-D can be seen to have the highest impact on the results, see Simulations 3.0 and 4.0. The most profitable scenario is combining FCR-D with peak shaving and energy arbitrage, Simulation 4.0, however, the difference between Simulation 3.0 with only FCR-D participation, and Simulation 4.0 where the battery is used for some energy arbitrage and peak shaving, is relatively small. Even though the maximum power decreases for 4.0 compared to 3.0, the costs for the maximum power are low compared to the other costs resulting in almost no effect on total costs.

As seen in the far right column, Simulation 1.2 is set as the base scenario for calculating the percentual difference, and not the first two scenarios with only a load or a load + solar production. This is to be able to compare how the optimization of the battery affects the results since all active components in 1.2 and 2.0 are the same except for the battery. Simulation 2.0 presents a 29% reduction in total costs, which is an increase in total revenue. The two last Simulations, 3.0 and 4.0, present a reduction in costs of more than 500% which further confirms the conclusion of the high revenues from ancillary services.

5.8 Sensitivity Analysis

To gain a better understanding of how the optimization can differentiate from the actual optimal solution, some investigations are performed for mainly the peak shaving and energy arbitrage optimization algorithm. First, the solution is compared with an algorithm more similar to a real-time control approach. Secondly, the weighting parameters are altered in order to understand what parameters affect for example the usage of the battery. Lastly, the FCR-D scenario is analyzed, as to how different percentages of accepted bids would affect the results obtained in Simulations 3.0 and 4.0.

5.8.1 Analysis 1 - Modifying weighting parameters in the objective function

To investigate how the solutions with the peak shaving and energy arbitrage optimization, Simulations 2.0 and 4.0 are impacted by different weighting these variables are altered and the results are compared. As written in Equation (4.2) the objective function consists of three different terms. The weighting variables γ modify the objective function to advance the behavior from one of the three terms. The choice of what weighting variables to adopt and present in analysis 2 are determined by the author's knowledge and thoughts when studying the resulting behaviour of the system depending on the size of the variables. However, many different weightings have been conducted in the model. Presented in Table 5.8, at least one case each of applying only one weight on one of the three terms when keeping the other weighting variables at 1 are simulated to see the impact of that one term in the objective function. One case when changing the variables a lot is also simulated to see if an extreme case affects the most (see row 4 in Table 5.8). All results are compared to the weighting adopted in previous simulations, this is shown in the last row in the table.

Table 5.8: Analysis of weighting parameters in the peak shaving and energy arbitrage optimization. The numbers are scaled with x, the simulations are run for January 2021.

Weigthing			**Nr of cycles**	**P_max**	**E_tot**	**C_var**	**C_p,max**	**C_tot**	**[%]**
γ_d	γ_b	γ_p	**over 31 days**	**[kW]**	**[kWh]**	**[SEK]**	**[SEK]**	**[SEK]**	
10	**1**	**1**	46	0.207x	67.4x	72x	17x	45x	+60.7%
100	**1**	**1**	54	0.335x	67.3x	73x	27x	60x	+114.3%
1	**10**	**1**	16	0.109x	66.2x	65x	9x	27x	−3.6%
0.1	**10e6**	**0.1**	0	0.167x	66.0x	67x	14x	36x	+28.6%
1	**1**	**10**	16	0.109x	66.3x	66x	9x	27x	−3.6%
1	**1**	**100**	16	0.109x	66.3x	66x	9x	27x	−3.6%
10	**1000**	**5**	15	0.109x	66.2x	65x	9x	28x	0

C_{char} and C_{fixed} are not shown in the table because they are constant for every simulation, same for C_{fcr} which is zero for this case.

Table 5.8 presents the analysis performed where the weighting is altered to weigh the three objective terms differently. If applying a higher weight on the first term, the day-ahead price will become more presiding i.e. the objective function will favor energy arbitrage. The second term in the equation aims to achieve stable usage of the battery without degrading its

lifespan due to many charge-discharge cycles. The third term of the objective function aims to minimize the maximum power bought directly from the grid, i.e. favor peak shaving.

From Table 5.8 it is presented that the total cost for high weight on the energy arbitrage term is not economically beneficial as opposed to high weighting on P_{max} that accounts for the lowest total cost. Even though all solutions approximately buy the same amount of energy from the grid (E_{tot}).

Figure 5.13, presents one simulation from the weighting analysis where the parameters were altered to benefit energy arbitrage and set to $\gamma_d = 100$ $\gamma_b = 1$ $\gamma_p = 1$.

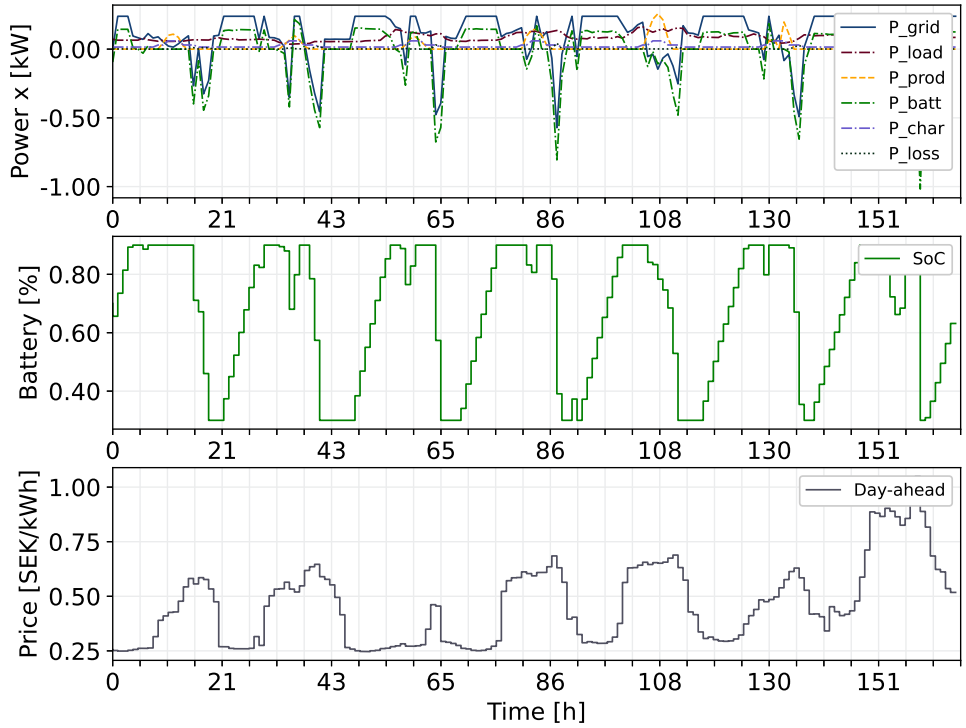

Figure 5.13: Results for the peak shaving and energy arbitrage optimization when the weighting parameters are $\gamma_d = 100$ $\gamma_b = 1$ $\gamma_p = 1$

In Figure 5.13, the negative peaks in P_{grid} and $P_{battery}$ display that more energy is being sold back to the grid, but the variable cost C_{var} is only a few x SEK higher for this weighting than for all other cases. This fortifies that energy arbitrage is not as economically beneficial as minimizing the maximum power input from the grid.

The behavior of Figure 5.13 is compared with the optimal control signals in Simulation 2.0 and Figure 5.7. From Figure 5.13 it is seen that the battery is charged when the day-ahead price is low and discharged when the price is at its highest every 24 hours. However, the fast charge and discharge together with no penalty on max power ($\gamma_p = 1$) lead to a higher cost of $C_{P,max}$, see Table 5.8 and more cycling of the battery.

5.8.2 Analysis 2 - Comparing optimal control with predictive control (MPC)

Simulation 2.0 with peak shaving and energy arbitrage is simulated to find what the optimal usage of the BESS could be. All necessary data is known in advance in that simulation, and the simulation is performed in one run. In reality, some kind of real-time control algorithm is used in an EMS for example MPC.

In order to estimate how reliable the results from the peak shaving optimization in Table 5.4 are, the result is compared with an implemented MPC algorithm. The optimization in the MPC is a bit different than for the other scenarios presented in Section 4.4.2. The MPC algorithm takes in the same data but optimizes only a smaller set, sends back the first optimal value, and then iterates through the specified time horizon and repeats with optimizing the control signals for every hour but by looking N hours in advance to make the optimal decision based on 12 hours, but then every hour the prediction moves one hour ahead.

Below is the outer algorithm that sends in vectors with N values of production, load, and the day-ahead price to simulate (Section 5.8.2) and then saves the returning optimal value only for the first hour, and then it repeats. For every new month, the maximum power bought from the grid is stored in a vector P_{max}.

Algorithm 1 MPC

Input: $P_{prod}, P_{cons}, C_{day-ahead}, Time$
Output: $SoC, P_{grid}, P_{battery}, P_{max}$
for $t \in Time$ **do**
$SoC, P_{grid}, P_{battery}, P_m \leftarrow simulate(SoC_{prev}, C_{day-ahead}, P_{prod}, P_{cons})$
$P_{max} \leftarrow \max(P_m, P_{max})$
end for

P_{prod}, P_{cons}, and $C_{day-ahead}$ are arrays with values $i = 1, 2, \ldots, N$ where N is the decided value of the prediction horizon.

Algorithm 2 simulate

Input: $N, \eta_c, \eta_t, U, R, SoC_{prev}, C_{day-ahead}, P_{prod}, P_{cons}$
Output: $SoC_{next}, P_{grid}[1], P_{battery}[1], P_{max}$
1: **minimize** $P_{grid} \cdot C_{day-ahead} + \Delta SoC + P_{max}$
2: $SoC[0] \leftarrow SoC_{prev}$
3: **for** $k \in N$ **do**
4: $P_{grid}[k] \leftarrow P_{battery}[k] - P_{prod}[k] + P_{cons}[k]$
5: **if** $P_{battery}[k] < 0$ **then**
6: $P_{grid} \leftarrow P_{battery} \cdot \eta_c \cdot \eta_t - P_{prod} \cdot \eta_t + P_{cons} \cdot \frac{1}{\eta_t}$
7: **else**
8: $P_{grid} \leftarrow P_{battery} \cdot \frac{1}{\eta_c \cdot \eta_t} - P_{prod} \cdot \eta_t + P_{cons} \cdot \frac{1}{\eta_t}$
9: **end if**
10: $P_{\text{loss}} \leftarrow R \cdot \frac{P_{battery}}{U^2}$
11: **if** $P_{battery} < 0$ **then**
12: $P_{batt} \leftarrow P_{battery} \cdot \eta_c \cdot \eta_t - P_{loss}$
13: **else**
14: $P_{batt} \leftarrow P_{battery} \frac{1}{\eta_c \cdot \eta_t} + P_{\text{loss}}$
15: **end if**
16: $SoC_{next} \leftarrow SoC + \frac{P_{batt}}{Q_b}$
17: $P_{lb} < P_{grid} < P_{max}$
18: $\Delta SoC \leftarrow SoC - SoC_{next}$
19: **end for**

Here the optimization works the same as for the energy arbitrage and peak shaving optimization but the inner algorithm optimizes only N number of hours and not the whole time horizon. Then the MPC iterates through the desired time but optimizes N number of values but saves only the first hour, since the next step one extra hour has become known so the prediction also iterates one hour forward, and then the first optimal value is saved and stored in the outer solution.

Since the day-ahead price is set 10-34 hours in advance, it is found reasonable to compare the optimal solution for peak shaving and energy arbitrage in Simulation 2.0 with different prediction horizons for the MPC solution. Table 5.9 presents the analysis performed where the prediction for the MPC is altered between 5-24 hours for one month, January 2021. The last row in the table shows the results for the earlier simulations with no MPC to be able to compare. C_charging and C_fixed are the same values for every simulation and C_fcr is zero for this case.

Table 5.9: Analysis of prediction horizons and the validity of the peak shaving optimization. The numbers are presented scaled with x, the simulation is run for one month, January 2021. The last row in the table shows the results for the earlier simulations with no MPC to be able to compare.

Prediction horizon	**Nr of cycles over 31 days**	**P_max [kW]**	**E_tot [kWh]**	**C_var [SEK]**	**C_p,max [SEK]**	**C_tot [SEK]**	**[%]**
N=5	8	0.178x	65.3x	64.3x	14.5x	32.9x	+22.8%
N=10	10	0.149x	65.4x	63.7x	12.2x	29.2x	+9.0%
N=15	11	0.131x	65.6x	63.9x	10.7x	27.7x	+3.4%
N=24	12	0.119x	65.7x	64.3x	9.7x	26.8x	0%
N=Hours	15	0.109x	66.2x	65.0x	8.9x	26.8x	0

From Table 5.9 it is seen that when only looking at 5 hours in advance, the total cost increases with 22% whilst 24 hours is seen to be successful in reaching the same optimal cost as by optimizing the whole time horizon in one iteration. This means the MPC has a very smart controller and that the prices do not differ that much to generate a different outcome of the total cost. The system is not so sensitive to fluctuations over the day. However, it is worth noting that the MPC does not contain predicted future data, which is more reliable to compare with.

Figure 5.14 and Figure 5.15 display the MPC with a prediction of 5 and 24 hours respectively.

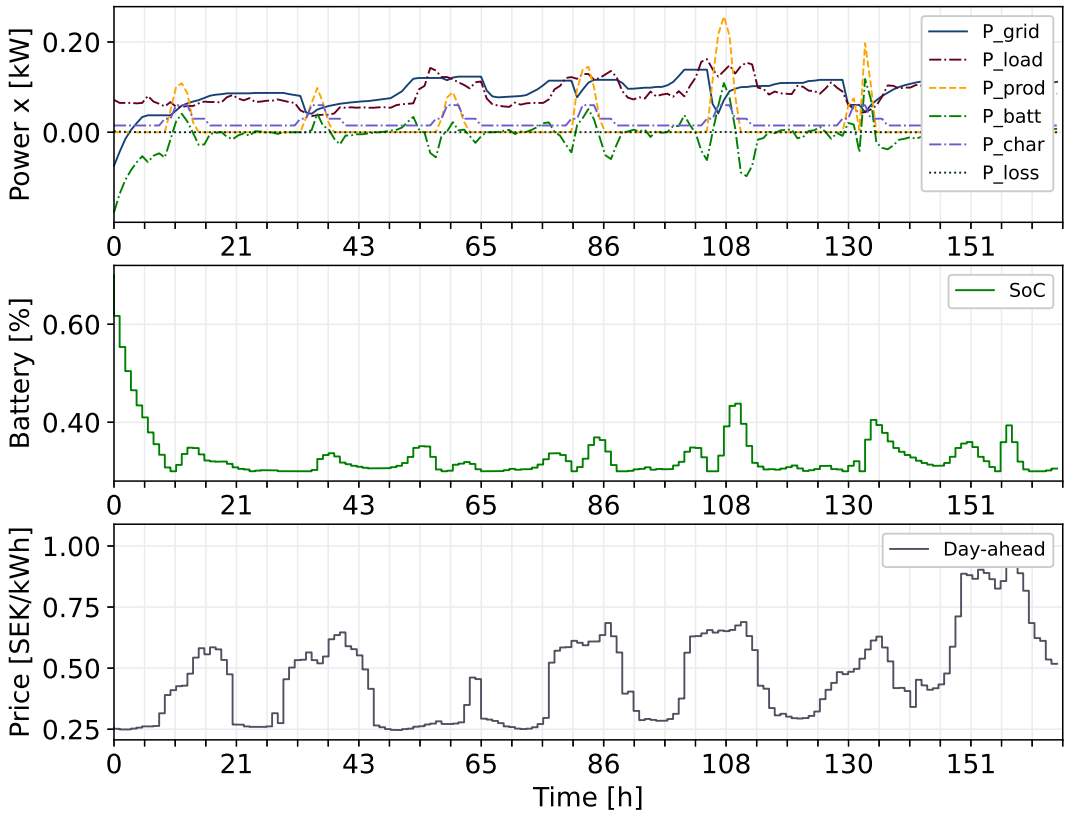

Figure 5.14: MPC for the energy arbitrage and peak shaving optimization, and prediction N=5 hours.

In Figure 5.14, P_{grid} reaches higher power output almost at the level of the load P_{load} and therefore does not provide as good peak shaving as for longer predictions. Furthermore, since the solver only looks 5 hours ahead, it does not see the benefits of charging the battery more when the day-ahead price is low and selling it when the price is at its highest, with a prediction horizon of 5 hours. The reason for this could be because the two terms of battery usage and peak power in the objective function affect the result a lot which makes the term for energy arbitrage in the objective function more subtle. This is further confirmed by Figure 5.13.

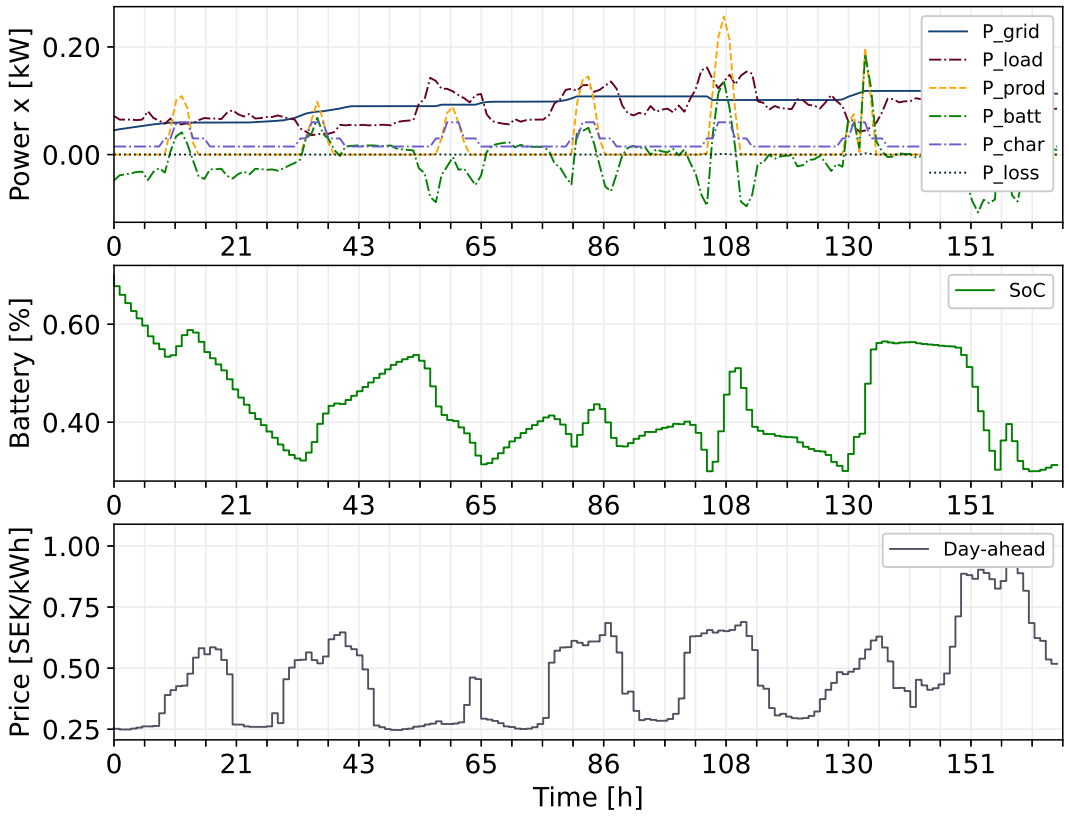

Figure 5.15: MPC for the energy arbitrage and peak shaving optimization, and prediction N=24 hours.

In Figure 5.15, P_{grid} remains at the same power output for 24 hours and then decides on the new optimal P_{max} that decides the new maximum level for the next P_{grid}. Furthermore, with a prediction of 24 hours, the solver charges and discharges the battery more similar to the optimal solution in Simulation 2.0 and Figure 5.7.

5.8.3 Analysis 3 - Altering day-ahead price and FCR-D remuneration

In the simulations, the day-ahead price of 2021 is used as opposed to the year 2022 because it was considered such an unusual year, see Section 4.2.4. However, if the day-ahead price would evolve to higher levels in the future energy arbitrage could become more beneficial. In addition, remuneration from ancillary services could deduct to lower price levels. Analysis 3 aims to investigate where these revenue streams from the different control techniques start to become more equivalent.

In Table 5.10, some of the previous yearly simulations are run with the day-ahead price and FCR-D remuneration of 2022 instead of 2021. As seen in Figure 4.4(a), the prices for 2022 are remarkably higher than for the year 2021. One case is simulated where the FCR-D remuneration of 2021 also decreased by 50% to represent a decline in remuneration in the future.

Table 5.10: Analysis of different hourly day-ahead prices and FCR-D remuneration during one year. The numbers are presented per unit x.

Simulation	Nr of cycles	P_max [kW]	E_tot [kWh]	C_var [SEK]	C_p,max [SEK]	C_fcr [SEK]	C_tot [SEK]	[%]
1.2	0	0.243x	-1 189x	-476x	146x	0x	-579x	0
2.0	338	0.147x	- 1 099x	-584x	60x	0x	-747x	−29%
3.0	0	0.243x	-1 189x	-476x	150x	-3 714x	-3 493x	−503%
1.2 - 2022	0	0.243x	-1 189x	-1 946x	146x	0x	-1 616x	−179%
2.0 - 2022	279	0.147x	-1 095x	-2 218x	70x	0x	-1 905x	−229%
3.0 - 2022	0	0.243x	-1 189x	-1 946x	150x	-5 230x	-5 732x	−890%
3.0 - 2021 -50%	0	0.243x	-1 189x	-476x	150x	-1 857x	-2 101x	−263%

From Table 5.10 it is clear that the higher electricity prices in the year 2022 lead to increased revenue for the arbitrage and peak shaving scenario. However, when looking at the difference in revenue in Simulations 1.0, 1.1, 1.2, and 2.0 for both 2021 and 2022, it is displayed that the increase in revenue for Simulations 1.1, 1.2, and 2.0 is still mainly derived from PV production. With the data of higher day-ahead prices from 2022, the increase in revenue from a battery is around 50 percentage units compared to Simulation 1.2 in 2022. The difference between 1.2 and 2.0 in 2021 was around 30 percentage units. This indicates that energy arbitrage is more beneficial in terms of revenue with more fluctuating energy prices. FCR-D revenue on the other hand impact the revenue more with higher remuneration and the simulation for the year 2022 shows an increased total revenue of around 890%. The analysis shows that it is hard to control the battery for energy arbitrage and obtain as much revenue as bidding on the FCR-D market. However, if the prices would decrease to 50% of the price level of the year 2021, energy arbitrage and peak shaving would start to become competitive.

6 Discussion

This chapter first introduces insights and outlooks derived from the comparison between the simulations performed. Secondly, the applied method is examined with the aim to highlight strengths and limitations as well as the impact on the results. Additionally, a discussion about the future of hybrid energy systems and ancillary services is provided along with suggestions for further work regarding the project topic.

6.1 Insights and outlook

The results of the simulations clearly showed that the highest revenue is based on the remuneration of the ancillary service FCR-D obtained from Svenska Kraftnät. This is affected by both the total available power to participate, the percentage of bids won, the remuneration prices, and the fee paid to the company responsible for the control, see Section 4.4.4 in Equation (4.6). In the simulation, the assumption of won bids was set to 50%. If this assumption would change to either higher or lower, it would affect the results a lot. A lower percentage of 25% would decrease the revenues for the remuneration in half, and an increase of won bids to 100% would increase the revenues to double. Since the remuneration for FCR-D played such a large part in the total costs, it is crucial to have a good bidding strategy and win as many bids as possible whilst at the same time achieving a high cost, see Section 2.1.1.2. The other parameters affecting this are also crucial but might be harder to modify since the power capacity is dependent on the invested size of the battery, the remuneration is decided by a third party and the fee to the control company is decided by the control company. What control company to use can however be chosen and the invested size of the battery can be smaller but kept at a higher level of SoC which can generate the same or a higher profit, especially if including the investment cost in the calculation. Moreover, if the remuneration from ancillary services keeps on increasing as Svenska Kraftnät has predicted shown in Figure 2.2, even more revenues can be expected. However, this is highly dependent on market forces, energy strategies, and governmental acts which is hard to predict.

Furthermore, the same factors will also affect the development of the day-ahead prices as well as the costs for peak power. If this changes drastically, the outcome could be different and the energy arbitrage and peak shaving scenario could be more beneficial than shown in this thesis, maybe even more beneficial than the scenario including remuneration from ancillary services. In some countries with a higher installed capacity from stationary batteries, the

remuneration from frequency containment reserves has declined over the last years. Instead, it has become more beneficial to control the BESS for energy arbitrage and peak shaving. This could be the future outlook in Sweden as well, when more capacity is bidding on the FCR-D market, the remuneration will most certainly drop. Together with a trend of rising energy usage, the costs for peak power and the day-ahead prices will most probably increase motivating companies more to work with energy arbitrage and peak shaving to save money.

Regarding the weighting in the objective function, Section 5.8.1, it was found that the weighting on the maximum power had the biggest impact on the optimal solution and resulted in the lowest cost. This can be explained by the fact that the cost for the maximum power is much higher than the variable costs and taxes, see Section 4.2.6 in Table 4.3. However, this will only impact the optimization of the objective function since the costs for the maximum power only provide one monthly additional cost in the calculation of the total cost. The weighting on the transferred electricity day-ahead price, the first term in the objective function presented in Section 4.4.2, actually made the solution worse when applying higher weight, that is when the solution acts more on buying electricity when the price is low and then selling it back when the price is high. It did although decrease the variable cost to some extent. Since the day-ahead price is quite low compared to the maximum power cost or the remuneration from FCR-D, this has little impact on the optimal solution.

The second sensitivity analysis showed that a prediction of 24 hours is beneficial in order to obtain a real-time control close to a yearly optimal solution. A shorter prediction horizon resulted in a worse control and higher cost, see Table 5.9. This is reasonable since when considering more data at every instance in the control loop, smarter decisions can be made. However, historical data is adopted which is not as accurate as predicted data. The results are likely to provide higher profit than if implementing prediction of the future input data. Although, the different energy holders in the model have very repetitive patterns and a machine-learning algorithm could probably achieve a reliable prediction for the majority of hours during the time simulated. As presented in Section 2.1.1.1, the costs are announced one day ahead at 14:00 which means the shortest prediction time based on the price is 10 hours. The simulated results showed that 10 hours of prediction generates values close to the optimal values. Since this is the shortest time to predict, and the longest time is 34 hours, the optimal values will be closer to the prediction time of 24 hours which concludes the controller in the system to be very smart in its decisions.

The last analysis with higher day-ahead prices and FCR-D remuneration strengthened the result that energy arbitrage is not as beneficial as participating at the FCR-D upmarket. However, more revenue from energy arbitrage is obtained when the day-ahead price is higher as well as fluctuates more throughout the day. The times the prices are a bit higher results in a higher cost for buying electricity while at the same time more earnings when selling. However, the difference in day-ahead price during one day is often only a few Swedish ore so the impact on the total cost becomes quite small in relation to the maximum power penalty and the FCR-D revenue in the objective function.

Overall, the results achieved in this study are specific to this system, its preconditions, and data. However, the results are similar to the results of related work and can therefore be seen as reliable.

6.2 Method review

In this subchapter, the project method is reviewed with important limitations and potential consequences from the assumptions that were made.

The system design was deeply influenced by an existing hybrid system. A wider design study could have been conducted to cover a variety of HES. In doing so, a broader understanding of the different design aspects could have been obtained. However, it would also result in a more general conclusion that perhaps would have been less applicable to the exact system investigated.

Furthermore, the stationary battery model created could have been developed to account for additional physical behaviors of the battery cells, but in accordance with adding complexity and computational cost to the model. For example, in Section 4.4.3 it is displayed that the internal losses are dependent on the variable power throughput in the battery, it is worth noting that the internal resistance of the battery, in reality, depends on multiple factors. Although the affecting of external factors is in most cases seen as low and establishing precise boundaries are required for modeling purposes.

Moreover, the simulations including the stationary battery implement a penalty (weighting) on the difference in SoC to make sure the optimal solution not charged/discharged the battery at a harmful rate. In this project, a harmful rate has been set to more than one full cycle per day, which is based on the literature research presented in Section 3.2. This assumption might not always be applicable. However, since large BESS in HES is relatively new, not enough research has been made on the degradation of the batteries to provide exact models of degradation due to batteries degrading differently depending on several external factors such as temperature, humidity, etc. Moreover, one full cycle is in this case set to the difference between the lower and the upper limit of SoC set in the battery multiplied by two, and not an entire cycle where the SoC reaches its minimum and maximum total capacity of 0 and 1. Additionally, the calculation of total cycles is based on the difference between every iteration independent of how large the difference is in every iteration. Both of these assumptions can be questioned further since the definition of one full cycle together with the amplitude of the difference in every iteration also might impact the degradation of the battery.

Regarding the simulations of the remuneration of ancillary services is limited to not including the activation of the specific reserve. This could affect the result since less power would be available in the BESS in case of an activation. Nonetheless, based on historical frequency data in the power grid shown in Section 4.2.5 in Table 4.2, an activation rarely occurs which ensures that the model choices and the results derived to be reliable.

The choice of optimization technique and software was heavily influenced by the authors' previous knowledge and university resources. While this may have provided a foundation for the study, it is important to acknowledge that there are numerous alternative approaches that could be as suitable for future research. To the author's knowledge, the simulation results would not differ that much by using another optimization technique or software.

Besides, the optimization relied on data from the years 2021 and 2022. To improve the robustness of the analysis and capture potential variations in our future outcomes to a greater extent, data could have been collected from a greater time span.

The sources in the project thesis were chosen based on how up-to-date they were as well as originating from well-recognized publishers, such as IEEE Xplore or ScienceDirect. By doing this, the aim was to make sure that the used information was reliable. However, it's important to recognize that there may still be limitations in the availability of diverse sources, and the sources selected could have their own biases. In the future, it would be valuable to explore a wider range of sources to get a more comprehensive understanding of the topic.

By critically examining these aspects of the study, the potential limitations and areas for improvement are acknowledged. These reflections provide insights for further studies in the modeling of hybrid energy systems, enabling more accurate project methods, and improved reliability of the results. However, the results from this study are still believed to be valid and reliable.

6.3 Further studies

The stationary battery could be modeled with multiple features to deeper the understanding regarding degradation such as further investigating losses, temperature effects, power throughput, and variable voltage among other factors.

In this project, the optimal control solution over a whole year was compared with a model predictive control algorithm to compare how close an actual real-time implementation can come to the optimal solution. However, the MPC could be evolved with the prediction of the energy demand and PV production as opposed to this project that relied on historical data. Although, even in reality when using prediction, historical data will be used to predict since the control algorithm cannot know exactly how much the sun will shine in the future, it can only predict and then adjust for the actual outcome.

Examining other ancillary services like Fast Frequency Response (FFR), Frequency Control Reserves - Normal (FCR-N), and FCR-D downward regulation, could be interesting to observe in order to create an even more promising business case for BESS installation and contributing to power grid stability.

Moreover, a comparative analysis of foreign ancillary markets could be valuable for gaining insights regarding the development of flexibility markets in Sweden.

The model can also be developed further to be able to show the breaking point between the profitability of ancillary services and the profitability of peak shaving and energy arbitrage in the same simulation instead of having to run different simulations.

To gain a better understanding of the economic feasibility related to HESs, the model can be extended with different perspectives regarding stakeholders' revenue models. For example, by exploring alternative pricing structures, examining different system architectures and where to place energy meters, and assessing the financial implications for different participants in the system. Furthermore, investment costs and levelized costs can be implemented in the model to make a deeper economic study to provide a better tool for the design of business models.

By pursuing these research directions, deeper knowledge with reference to hybrid energy systems and energy management systems can be obtained. The outcomes of such studies will not only enhance the theoretical foundation but also contribute to the installation and operation of these systems, hopefully leading to more renewable energy and efficient energy utilization.

7 Conclusion

This chapter provides a summary of the purpose of the study as well as addresses the research questions. We have also shared our key findings and insights. Additionally, a conclusion of suggestions for future work in the field is presented.

7.1 Conclusion

In conclusion, the focus of this project has been to implement a model with an optimization algorithm for a Hybrid Energy System containing of a load, photovoltaics, charging stations, and a stationary battery. To validate the model, different simulations were performed. First, without the battery and in doing so create a baseline for comparison. Secondly, controlling the battery for energy arbitrage and peak shaving optimization. Lastly, controlling the battery for participating in the Swedish balancing market frequency containment reserve upwards regulation. The simulations presented different costs and revenues as well as important control signals such as the state of charge of the battery or assumptions regarding accepted bids on FCR-D.

The sensitivity analysis for the arbitrage and peak shaving optimization showed that the weighting of the three terms in the objective function had a high impact on the total results. A high weight on the energy arbitrage term decreased the variable cost a little, but contrary to the purpose, it increased the peak power since more energy was transferred to and from the grid at every hour. It also impacted the number of cycles negatively and the penalty on the variation in the state of charge was important to keep the total amount of cycles below 1 cycle per day on average. Although, a too-high penalty on ΔSoC made the battery not contribute at all and caused a less optimal solution. Applying high weight to the maximum power had a better impact on the total revenue. But the maximum power could only be minimized to a certain level, some energy still has to be bought to account for the load when the photovoltaic production is low.

The insights and outlook derived from the simulations showed that the energy arbitrage strategy only reduced the cost to some extent, the same result was obtained with the higher electricity prices of the year 2022. If the prices would fluctuate more from day to day, arbitrage would most likely be a bit more economically beneficial, but to the cost of more battery degradation. The main reduction in cost for the arbitrage and peak shaving scenario was achieved by implementing a penalty in the objective function on the maximum power bought from the

grid. This is reasonable since this reduces the maximum power peaks which accounts for the highest electricity subscription cost every month.

However, the arbitrage and peak shaving Simulations was not as remarkable as the increase in revenue when participating in the FCR-D market. On top of this, the Simulation 3.0 and 4.0 presented less cycling of the battery. The FCR-D bidding would still account for the highest revenue even if the remuneration decreased by 50% from the year 2021. Although, if the total bidding volume becomes greater in the future as more batteries are connected to the balancing market, the result could differ since it becomes harder to remain as one of the accepted bids every hour.

In conclusion, the optimal usage of a Battery Energy Storage System for years 2021 and 2022 has been to participate in the FCR-D upmarket and keep the battery state of charge at a constant charge which also causes minimal degradation to the battery. Overall, the simulations provide valuable insights into the performance of different control scenarios and can be used to optimize the operation of energy management systems in the future.

7.2 Future work

The authors have identified a few areas for future work in the field of Hybrid Energy Systems, described in Section 6.3, these include:

- Enhancing the modeling of stationary batteries
- Incorporating real-time prediction in the control algorithm
- Exploring additional ancillary services
- Conducting comparative analyses of foreign balancing markets

Pursuing these research directions will contribute to a deeper understanding of hybrid energy systems, improve their practical implementation, and promote the use of renewable energy and efficient energy utilization.

Bibliography

[1] Md Masud Rana et al. "A review on hybrid photovoltaic – Battery energy storage system: Current status, challenges, and future directions". In: *Journal of Energy Storage* 51 (2022), p. 104597. ISSN: 2352-152X. DOI: https://doi.org/10.1016/j.est.2022.104597.

[2] M. Reza et al. "Optimal Algorithms for Energy Storage Systems in Microgrid Applications: An Analytical Evaluation Towards Future Directions". In: *IEEE Access* 10 (Jan. 2022), pp. 1–1. DOI: 10.1109/ACCESS.2022.3144930.

[3] Marc Möller et al. "SimSES: A holistic simulation framework for modeling and analyzing stationary energy storage systems". In: *Journal of Energy Storage* 49 (2022), p. 103743. ISSN: 2352-152X. DOI: https://doi.org/10.1016/j.est.2021.103743.

[4] Jonathan Ullmark et al. "Inclusion of frequency control constraints in energy system investment modeling". In: *Renewable Energy* 173 (2021), pp. 249–262. DOI: https://doi.org/10.1016/j.renene.2021.03.114.

[5] Heejung Park. "A Stochastic Planning Model for Battery Energy Storage Systems Coupled with Utility-Scale Solar Photovoltaics". In: *Energies* 14 (Feb. 2021), p. 1244. DOI: 10.3390/en14051244.

[6] Raymond Byrne et al. "Energy Management and Optimization Methods for Grid Energy Storage Systems". In: *IEEE Access* PP (Aug. 2017), pp. 1–1. DOI: 10.1109/ACCESS.2017.2741578.

[7] Jonas Engels et al. "Combined Stochastic Optimization of Frequency Control and Self-Consumption With a Battery". In: *IEEE Transactions on Smart Grid* 10.2 (2019), pp. 1971–1981. DOI: 10.1109/TSG.2017.2785040.

[8] SvenskaKraftnat. *Frekvenshallningsreserv storning uppreglering (FCR-D upp)*. https://www.svk.se/aktorsportalen/bidra-med-reserver/om-olika-reserver/fcr-d-upp/. Accessed on February 2, 2023.

[9] Swedish Energy Agency. *Energy in Sweden 2022 - An overview*. https://www.energimyndigheten.se/en/news/2022/an-overview-of-energy-in-sweden-2022-now-available/. Accessed on March 30, 2023. 2022.

[10] Svenska kraftnät. *Sveriges elnät*. https://www.svk.se/om-kraftsystemet/oversikt-av-kraftsystemet/sveriges-elnat/. Accessed on March 30, 2023.

[11] Svenska kraftnät. *Anslutning till transmissionsnätet*. https://www.svk.se/om-kraftsystemet/om-systemansvaret/verktyg-for-systemdrift/anslutning-till-transmissionsnatet/. Accessed on March 30, 2023.

[12] Svenska kraftnät. *Reliable electricity supply*. https://www.svk.se/en/national-grid/reliable-electricity-supply/. 2021.

[13] Svenska kraftnät. *Operations and electricity markets*. https://www.svk.se/en/national-grid/operations-and-electricity-markets/. 2021.

[14] Md N. H. Shazon and Abdul Jawad. "Frequency control challenges and potential countermeasures in future low-inertia power systems: A review". In: *Energy Reports* 8 (2022), pp. 6191–6219. DOI: 10.1016/j.egyr.2022.04.063.

[15] M. H. Shakil et al. "Transmission expansion planning considering renewable energy sources: A review". In: *Renewable and Sustainable Energy Reviews* 134 (2020), p. 110249. ISSN: 1364-0321. DOI: 10.1016/j.rser.2020.110249.

[16] Svenska kraftnät. *Om olika reserver*. https://www.svk.se/aktorsportalen/bidra-med-reserver/om-olika-reserver/. Accessed on March, 30 2023.

[17] SvenskaKraftnat. "Systemutvecklingsplan2022–2031". In: *Systemutvecklingsplan2022-2031* 1.1 (2022), p. 151.

[18] Zeenat Hameed et al. "Investigating the participation of battery energy storage systems in the Nordic ancillary services markets from a business perspective". In: *Journal of Energy Storage* 58 (2023), p. 106464. DOI: https://doi.org/10.1016/j.est.2022.106464.

[19] Jan Figgener et al. "The development of stationary battery storage systems in Germany–A market review". In: *Journal of energy storage* 29 (2020), p. 101153. DOI: https://doi.org/10.1016/j.est.2019.101153.

[20] SvenskaKraftnät. *Marknaden för stödtjänster till kraftsystemet växer kraftigt*. https://www.svk.se/press-och-nyheter/press/marknaden-for-stodtjanster-till-kraftsystemet-vaxer-kraftigt---3292104/. Accessed on April 14, 2023.

[21] Yuanyuan Shi et al. "Using Battery Storage for Peak Shaving and Frequency Regulation: Joint Optimization for Superlinear Gains". In: *IEEE Transactions on Power Systems* 33.3 (2018), pp. 2882–2894. DOI: 10.1109/TPWRS.2017.2749512.

[22] Raphael Hollinger et al. "Fast Frequency Response with BESS: A Comparative Analysis of Germany, Great Britain and Sweden". In: *2018 15th International Conference on the European Energy Market (EEM)*. 2018, pp. 1–6. DOI: 10.1109/EEM.2018.8469998.

[23] Yuan-Kang Wu and Kuo-Ting Tang. "Frequency support by BESS–Review and analysis". In: *Energy Procedia* 156 (2019), pp. 187–191. DOI: https://doi.org/10.1016/j.egypro.2018.11.126.

[24] Power Circle. *Lokala energilager i distributionsnäten*. https://powercircle.org/lokala-energilager-i-distributionsnaten/. Accessed on March, 31 2023. 2016.

[25] Junhee Kim et al. "A simple operating strategy of small-scale battery energy storages for energy arbitrage under dynamic pricing tariffs". In: *IEEE Transactions on Smart Grid* 8.6 (2016), pp. 3031–3041. DOI: https://doi.org/10.3390/en9010012.

[26] A. Rahimi et al. "A simple and effective approach for peak load shaving using Battery Storage Systems". In: *2013 North American Power Symposium (NAPS)*. 2013, pp. 1–5. DOI: 10.1109/NAPS.2013.6666824.

[27] Vattenfall. *Vad består min elkostnad av?* https://www.vattenfall.se/fokus/tips-rad/vad-bestar-elkostnad-av/. 2023.

[28] Kraftringen Energi. *Producera egen el*. https://www.kraftringen.se/privat/el/elnat/producera-egen-el/. Accessed on May 2, 2023. 2023.

[29] Arechkik Ameur et al. "Chapter 6 - Performance and energetic modeling of hybrid PV systems coupled with battery energy storage". In: *Hybrid Energy System Models*. Ed. by Asmae Berrada and Rachid El Mrabet. Academic Press, 2021, pp. 195–238. ISBN: 978-0-12-821403-9. DOI: https://doi.org/10.1016/B978-0-12-821403-9.00008-1.

[30] Roberto Faranda, Sonia Leva, et al. "Energy comparison of MPPT techniques for PV Systems". In: *WSEAS transactions on power systems* 3.6 (2008), pp. 446–455.

[31] Amy Miele et al. "The role of charging and refuelling infrastructure in supporting zero-emission vehicle sales". In: *Transportation Research Part D: Transport and Environment* 81 (2020), p. 102275. DOI: 10.1016/j.trd.2020.102275.

[32] Elbilsstatistik. *Laddinfrastrukturstatistik*. https://www.elbilsstatistik.se/laddinfrastatistik. Accessed on April 11, 2023.

[33] Camilo Suarez and Wilmar Martinez. "Fast and Ultra-Fast Charging for Battery Electric Vehicles – A Review". In: *2019 IEEE Energy Conversion Congress and Exposition (ECCE)*. 2019, pp. 569–575. DOI: 10.1109/ECCE.2019.8912594.

[34] Miljöförvaltningen Stockholm. *Kvantitativ analys av nyttjandet av publika laddplatser i Stockholm stad under perioden 4Q2015-3Q2016*. Rapport. Stockholms stad, 2021.

[35] Miljöförvaltningen. *Kvantitativ analys av nyttjandet av publika laddplatser i Stockholm stad under perioden 4Q2015-3Q2016*. Technical Report. 2016.

[36] Mobility Sweden. *Elprisanalys 2022*. https://mobilitysweden.se/aktuellt/i-debatten/pressmeddelanden/elbilen-fortsatt-billigast-trots-hoga-elpriser. Accessed April 24, 2023. 2022.

[37] OKQ8. *Kostnad ladda elbil*. https://www.okq8.se/elbilsladdning/kostnad-ladda-elbil/. Accessed April 24, 2023.

[38] Göteborg Energi. *Vad kostar det att ladda?* https://www.goteborgenergi.se/privat/ladda-elbil/vad-kostar-det. Accessed April 24, 2023.

[39] Mereco. *Prislista publik laddning*. https://se.mer.eco/laddstationer/priser/. Accessed April 24, 2023.

[40] Steffen Limmer. "Dynamic Pricing for Electric Vehicle Charging—A Literature Review". In: *Energies* 12.18 (2019). ISSN: 1996-1073. DOI: 10.3390/en12183574.

[41] Abdeslem Kadri and Kaamran Raahemifar. "Optimal Sizing and Scheduling of Battery Storage System Incorporated with PV for Energy Arbitrage in Three Different Electricity Markets". In: *2019 IEEE Canadian Conference of Electrical and Computer Engineering (CCECE)*. 2019, pp. 1–6. DOI: 10.1109/CCECE.2019.8861776.

[42] Philipp Schreiber et al. "Photovoltaics and battery storage—Python-based optimisation for innovation tenders". In: *Proceedings of the International Renewable Energy Storage Conference 2021 (IRES 2021)*. Atlantis Press, 2022, pp. 100–107. ISBN: 978-94-6239-546-6. DOI: 10.2991/ahe.k.220301.010.

[43] Ke Jia et al. "Historical-data-based energy management in a microgrid with a hybrid energy storage system". In: *IEEE Transactions on Industrial Informatics* 13.5 (2017), pp. 2597–2605. DOI: 10.1109/TII.2017.2700463.

[44] Bolun Xu et al. "Optimal Battery Participation in Frequency Regulation Markets". In: *IEEE Transactions on Power Systems* 33.6 (2018), pp. 6715–6725. DOI: 10.1109/TPWRS.2018.2846774.

[45] Philipp Fortenbacher et al. "Modeling and Optimal Operation of Distributed Battery Storage in Low Voltage Grids". In: *IEEE Transactions on Power Systems* 32.6 (2017), pp. 4340–4350. DOI: 10.1109/TPWRS.2017.2682339.

[46] Yi Li et al. "Data-driven health estimation and lifetime prediction of lithium-ion batteries: A review". In: *Renewable and Sustainable Energy Reviews* 113 (2019), p. 109254. ISSN: 1364-0321. DOI: https://doi.org/10.1016/j.rser.2019.109254.

[47] Christine Harnischmacher et al. "Two-sided sustainability: Simulating battery degradation in vehicle to grid applications within autonomous electric port transportation". In: *Journal of Cleaner Production* 384 (2023), p. 135598. ISSN: 0959-6526. DOI: https://doi.org/10.1016/j.jclepro.2022.135598.

[48] Rui Xie et al. "BESS frequency regulation strategy on the constraints of planned energy arbitrage using chance-constrained programming". In: *Energy Reports* 8 (2022). 2022 The 4th International Conference on Clean Energy and Electrical Systems, pp. 73–80. ISSN: 2352-4847. DOI: https://doi.org/10.1016/j.egyr.2022.05.129.

[49] Bolong Cheng and Warren B. Powell. "Co-Optimizing Battery Storage for the Frequency Regulation and Energy Arbitrage Using Multi-Scale Dynamic Programming". In: *IEEE Transactions on Smart Grid* 9.3 (2018), pp. 1997–2005. DOI: 10.1109/TSG.2016.2605141.

[50] A. Aguilera-Gonzalez et al. "Model Predictive Control for Optimal Energy Management of an Island Wind Storage Hybrid Power Plant". In: *IFAC-PapersOnLine* 53.2 (2020). 21st IFAC World Congress, pp. 12841–12846. ISSN: 2405-8963. DOI: https://doi.org/10.1016/j.ifacol.2020.12.1982.

[51] Christofer Sundström et al. "Analysis of optimal energy management in smart homes using MPC". In: *2016 European Control Conference (ECC)*. 2016, pp. 2066–2071. DOI: 10.1109/ECC.2016.7810596.

[52] Rama K. Bonthu et al. "Energy Cost Optimization in Microgrids Using Model Predictive Control and Mixed Integer Linear Programming". In: *2019 IEEE International Conference on Industrial Technology (ICIT)*. 2019, pp. 1113–1118. DOI: 10.1109/ICIT.2019.8754971.

[53] The Green Watt. *How to Calculate Solar Panel Output*. https://thegreenwatt.com/how-to-calculate-solar-panel-output/. Accessed on May 16, 2023.

[54] Lucas Xavier et al. "Power converters for battery energy storage systems connected to medium voltage systems: a comprehensive review". In: *BMC Energy* 1 (July 2019). DOI: 10.1186/s42500-019-0006-5.

[55] MIT. *MIT Electric Vehicle Team - What do battery specifications actually mean?* https://web.mit.edu/evt/info.html. Accessed on May 16, 2023.

[56] Elena M. Krieger and Craig B. Arnold. "Effects of undercharge and internal loss on the rate dependence of battery charge storage efficiency". In: *Journal of Power Sources* 210 (2012), pp. 286–291. ISSN: 0378-7753. DOI: https://doi.org/10.1016/j.jpowsour.2012.03.029.

[57] Elpiniki Apostolaki-Iosifidou et al. "Measurement of power loss during electric vehicle charging and discharging". In: *Energy* 127 (2017), pp. 730–742. ISSN: 0360-5442. DOI: https://doi.org/10.1016/j.energy.2017.03.015.

[58] R Rakshitha. "Integration of Coulomb Counting Method in Battery Management System for Electric Vehicle". In: *International Journal of Engineering Research and* V9 (May 2020). DOI: 10.17577/IJERTV9IS050639.

[59] Annette E. Trippe et al. "Charging optimization of battery electric vehicles including cycle battery aging". In: *IEEE PES Innovative Smart Grid Technologies, Europe*. 2014, pp. 1–6. DOI: 10.1109/ISGTEurope.2014.7028735.

[60] W. Waag and D.U. Sauer. "SECONDARY BATTERIES – LEAD– ACID SYSTEMS | State-of-Charge/Health". In: *Encyclopedia of Electrochemical Power Sources*. Ed. by Jürgen Garche. Amsterdam: Elsevier, 2009, pp. 793–804. ISBN: 978-0-444-52745-5. DOI: https://doi.org/10.1016/B978-044452745-5.00149-0.

[61] Kubra Nur Akpinar et al. "A novel cycle counting perspective for energy management of grid integrated battery energy storage systems". In: *Energy Reports* 9 (2023). 2022 9th International Conference on Power and Energy Systems Engineering, pp. 123–131. ISSN: 2352-4847. DOI: https://doi.org/10.1016/j.egyr.2022.10.359.

[62] Yung-Li Lee et al. *Metal fatigue analysis handbook: practical problem-solving techniques for computer-aided engineering*. Elsevier, 2011.

[63] George Bernard Dantzig and Mukund N Thapa. *Linear programming: Theory and extensions*. Vol. 2. Springer, 2003.

[64] Fabian Huneke et al. "Optimisation of hybrid off-grid energy systems by linear programming". In: *Energy, Sustainability and Society* 2.1 (2012), pp. 1–19.

[65] Dimitris Bertsimas and John N Tsitsiklis. *Introduction to linear optimization*. Athena Scientific, 1997.

[66] Chouaib Ammari et al. "Sizing, optimization, control and energy management of hybrid renewable energy system—A review". In: *Energy and Built Environment* 3.4 (2022), pp. 399–411. DOI: https://doi.org/10.1016/j.enbenv.2021.04.002.

[67] K Holmberg. *Optimering - metoder, modeller och teori för linjära, olinjära och kombinatoriska problem*. Vol. 2:1. Liber AB: Kina, 2010.

[68] Luu Ngoc An and Tran Quoc Tuan. "Dynamic programming for optimal energy management of hybrid wind–PV–diesel–battery". In: *Energies* 11.11 (2018), p. 3039. DOI: 10.3390/en11113039.

[69] UKEssays. *Linear Programming: Advantages, Disadvantages and Strategies*. Accessed on April 14, 2023. 2018.

[70] MathWorks. *What is Model Predictive Control (MPC)?* https://www.mathworks.com/help/mpc/gs/what-is-mpc.html. Accessed 2023-04-17.

[71] ENTSO-E. *ENTSO-E Day-Ahead Prices*. https://transparency.entsoe.eu/. Accessed on April 14, 2023.

[72] SvenskaKraftnät. *Primary Regulation Market Data*. https://mimer.svk.se/PrimaryRegulation/PrimaryRegulationIndex. Accessed on April 14, 2023.

[73] Genas, S and Karlén, A. *Margins for tomorrow: A quantitative analysis of the flexibility from aggregated electric vehicles*. https://www.diva-portal.org/smash/get/diva2:1580044/FULLTEXT01.pdf. Accessed on May 3, 2023. 2021.